

GEM – An Energy Conserving Electromagnetic Gyrofluid Model

Bruce D. Scott*

Max-Planck-Institut für Plasmaphysik, Euratom Association, D-85748 Garching, Germany

(Dated: October 25, 2018)

The details of fluctuation free energy conservation in the gyrofluid model are examined. The polarisation equation relates ExB flow and eddy energy to combinations of the potential and the density and perpendicular temperature. These determine the combinations which must appear under derivatives in the moment equations so that not only thermal free energy but its combination with the ExB energy is properly conserved by parallel and perpendicular compressional effects. The resulting system exhibits the same qualitative energy transfer properties as corresponding Braginskii or Landau fluid models. One clear result is that the numerical model built on these equations is well behaved for arbitrarily large perpendicular wavenumber, allowing exploration of two scale phenomena linking dynamics at the ion and electron gyroradii. When the numerical formulation is done in the globally consistent flux tube model, the results with adiabatic electrons are consistent with the “Cyclone Base Case” results of gyrokinetic models.

PACS numbers: 52.65.Tt, 52.35.Ra, 52.30.-q, 52.25.Fi

I. INTRODUCTION – GYROFLUID ENERGY CONSERVATION IN GENERAL

Gyrofluid models, whose most prominent application has been to tokamak core turbulence as exemplified by the Cyclone Base Case [1], were originally constructed to incorporate finite ion gyroradius effects at arbitrary order into simple computations of turbulence occurring in largely two dimensional fluid experiments [2]. To treat ion temperature gradient (ITG) turbulence the temperatures were incorporated and the model acquired several new advection terms, producing nonlinearities as well as drift frequency corrections, resulting from the effect of temperature fluctuations on the gyroaveraging operator [3, 4]. However, although the nonlinearities were incorporated, much of the analysis involved linear frequencies and growth rates and the nonlinearities were added largely as an afterthought. Specifically, there was no complete energetic analysis of the type familiar from drift wave turbulence work [5, 6, 7, 8]. The GEM model was introduced previously in the context of energetic considerations, including the correspondence between fluid drift and gyrofluid models under drift ordering [9]. We develop the energetics for the six-moment model including temperature and parallel heat flux dynamics herein, placing this model on a secure energetic footing for the first time.

Under drift ordering [10], this energetics involves “fluctuation free energy,” in which the thermal free energy enters as the average squared amplitude of the density fluctuations [5], with additional contributions from the average squared amplitude of the temperature fluctuations in the appropriately generalised models [7]. The rest of the free energy is made up of contributions due to the ExB energy involving the electrostatic potential, the magnetic energy involving the parallel magnetic potential, and the parallel free energy in not only the parallel velocities but also the parallel heat fluxes [8]. A properly constructed model should conserve this free energy in all processes except those involving clearly identifiable sources (gradients) and sinks (dissipative processes such as resistivity, thermal conduction, or Landau damping). Many models neglect this consideration because small errors in the energetics lead simply to negligible contributions to the growth rate in a linear model. However, if the model is to be useful in a turbulent setting, the energetics must be consistent in order to achieve a reliable saturated state in which the salient energetic processes and the turbulent transport can be statistically measured.

The processes linking the thermal free energy to the ExB turbulence are of physical importance because the free energy sources and sinks are not in the perpendicular equation of motion. The energy source given by the general profile gradient, is in the equations for the thermal state variables (density, temperatures). The dissipation processes are in the equations for the parallel flux variables (current, heat fluxes). In saturation, the ExB energy itself is maintained as a statistical balance between various conservative transfer effects which connect to these sources and sinks in the other parts of the dynamics (this neglects certain rotation damping processes which are often not considered). In this balance it is important that the conservative nature of such processes such as shear Alfvén dynamics or interchange effects is maintained in the model. The simplest example is an isothermal two dimensional magnetohydrodynamical

*email: bds@ipp.mpg.de;

URL: <http://www.rzg.mpg.de/~bds/>

(MHD) interchange model, given by

$$\frac{n_i M_i c^2}{B^2} \frac{\partial}{\partial t} \nabla_{\perp}^2 \tilde{\phi} = -T_e \mathcal{K}(\tilde{n}_e) \quad (1)$$

$$\frac{\partial \tilde{n}_e}{\partial t} + \mathbf{v}_E \cdot \nabla (n_e + \tilde{n}_e) = n_e \mathcal{K}(\tilde{\phi}) \quad (2)$$

where the perpendicular Laplacian and curvature operator are defined by

$$\nabla_{\perp}^2 = -\nabla \cdot [\mathbf{b} \times (\mathbf{b} \times \nabla)] \quad (3)$$

$$\mathcal{K} = \nabla \cdot \left[\frac{c}{B^2} (\mathbf{B} \times \nabla) \right] \quad (4)$$

respectively, with $\mathbf{B} = B\mathbf{b}$ the equilibrium magnetic field. The ExB velocity is given by

$$\mathbf{v}_E = \frac{c}{B} \mathbf{b} \times \nabla \tilde{\phi} \quad (5)$$

The curvature terms in Eqs. (1,2) respectively represent quasistatic compression of the diamagnetic current and the ExB velocity.

Under drift ordering [10], the background parameters are constants except where operated upon by $\mathbf{v}_E \cdot \nabla$, the ExB advection. The magnetic field is treated as constant except for the existence of $\mathcal{K}()$. In the advection term, the velocity \mathbf{v}_E is treated as divergence free; the finite ExB divergence is accounted for by $\mathcal{K}(\tilde{\phi})$. If we multiply these equations by $-\tilde{\phi}$ and $(T_e/n_e)\tilde{n}_e$, respectively, and integrate over the entire spatial domain, we find, neglecting surface terms,

$$\frac{\partial}{\partial t} \int d\Lambda \frac{n_i M_i c^2}{2} \frac{c^2}{B^2} |\nabla_{\perp} \tilde{\phi}|^2 = - \int d\Lambda T_e \tilde{n}_e \mathcal{K}(\tilde{\phi}) \quad (6)$$

$$\frac{\partial}{\partial t} \int d\Lambda \frac{n_e T_e}{2} \left(\frac{\tilde{n}_e}{n_e} \right)^2 = - \int d\Lambda T_e \tilde{n}_e \mathbf{v}_E \cdot \nabla \log n_e + \int d\Lambda T_e \tilde{n}_e \mathcal{K}(\tilde{\phi}) \quad (7)$$

where $\int d\Lambda$ by itself gives the total volume. These two lines give the evolution of the ExB drift and thermal free energy, respectively. The interchange effect represented by $\mathcal{K}()$ transfers free energy between these two pieces conservatively, as we would expect from a compressional process, because $\mathcal{K}()$ is at once a total divergence and a first order linear differential operator. The source is given by the advection of the background gradient, proportional to the average flux. This model will saturate only if there is a loss process at the boundary, or some nonlinear effect enters to cause the source to go to zero, or some additional effect is considered in the model by which an explicit sink term appears to balance the source (a detailed analysis of how this functions in a three dimensional drift Alfvén model is given in Ref. [8]).

In a gyrofluid model, there is no equation for the vorticity explicitly involving time derivatives. Instead, at the same level of sophistication as above, there is an evolution equation for each of the species' gyrocenter densities, as opposed to space densities. In each density equation, the potential is gyroaveraged using a suitable convolution operator which is described by a kernel in Fourier space:

$$\tilde{\phi}_G = G(\tilde{\phi}) = \sum_{\mathbf{k}_{\perp}} G_{\mathbf{k}_{\perp}} \tilde{\phi}_{\mathbf{k}_{\perp}} e^{i\mathbf{k}_{\perp} \cdot \mathbf{x}} \quad (8)$$

The usual form for $G_{\mathbf{k}_{\perp}}$ is $\Gamma_0^{1/2}(b_i)$, which is an average of the single particle form $J_0(k_{\perp} v_{\perp} / \Omega_i)$ averaged over the perturbed distribution function [3]. The argument is $b_i = k_{\perp}^2 \rho_i^2$, where ρ_i is the thermal gyroradius and Ω_i is the gyrofrequency. Unless phenomena below the ion scale ρ_i are considered, electron gyroradius effects are usually ignored, so that $G_{\mathbf{k}_{\perp}} = 1$ for them. The potential is given by a polarisation equation which equates the two space densities, each given by a combination of the gyrocenter and polarisation densities, the latter involving the gyroscreened potential. The equations appear as [2]:

$$\frac{\partial \tilde{n}_e}{\partial t} + \mathbf{v}_E \cdot \nabla (n_e + \tilde{n}_e) = n_e \mathcal{K}(\tilde{\phi}) - \frac{T_e}{e} \mathcal{K}(\tilde{n}_e) \quad (9)$$

$$\frac{\partial \tilde{n}_i}{\partial t} + \mathbf{u}_E \cdot \nabla (n_i + \tilde{n}_i) = n_i \mathcal{K}(\tilde{\phi}_G) + \frac{T_i}{e} \mathcal{K}(\tilde{n}_i) \quad (10)$$

$$\frac{G(\tilde{n}_i)}{n_i} + \frac{e}{T_i} \rho_i^2 \nabla_{\perp}^2 \tilde{\phi} = \frac{\tilde{n}_e}{n_e} \quad (11)$$

Gyroscreening is distinct from gyroaveraging; in general this is given by another operator whose usual kernel in \mathbf{k}_{\perp} -space is $\Gamma_0(b_i) - 1$. The low- k_{\perp} form of this is just $-b_i$, which in real space yields the $\rho_i^2 \nabla_{\perp}^2$ form used in Eq. 11.

It is important to note however that the same operator is involved in the gyroaveraging of the potential (Eq. 8) as in the conversion of the gyrocenter density, \tilde{n}_i , to the ion space density given by the left side of Eq. (11). For the ions, the operator is G ; for the electrons, it is unity. Consistent with this, the ExB advection of the ion density occurs with the gyroaveraged potential, with velocity

$$\mathbf{u}_E = \frac{c}{B} \mathbf{b} \times \nabla \tilde{\phi}_G \quad (12)$$

while the electrons are advected by the “bare” version, the same \mathbf{v}_E as in Eq. (5). The curvature operator acts on the total force potential of each species, respectively, i.e., the diamagnetic velocity divergences are necessarily kept in the model, which cannot take the MHD form if both pressures are to contribute to charge separation.

The point to be made here is the way in which the polarisation equation, Eq. (11), determines the acceptable form for many of the differential operators in the moment equations. The ExB energy and the electron and ion thermal free energies are given by

$$U_E = \int d\Lambda \frac{n_i M_i}{2} \frac{c^2}{B^2} |\nabla_{\perp} \tilde{\phi}|^2 \quad U_e = \int d\Lambda \frac{n_e T_e}{2} \left(\frac{\tilde{n}_e}{n_e} \right)^2 \quad U_i = \int d\Lambda \frac{n_i T_i}{2} \left(\frac{\tilde{n}_i}{n_i} \right)^2 \quad (13)$$

respectively. Using Eq. (11) and the Hermitian property of G , we may recast U_E as

$$U_E = e \frac{\tilde{\phi}_G \tilde{n}_i}{2} - e \frac{\tilde{\phi} \tilde{n}_e}{2} \quad (14)$$

which shows the ion and electron contributions separately. By similar means, the time derivatives are given by

$$\frac{\partial U_E}{\partial t} = e \tilde{\phi}_G \frac{\partial \tilde{n}_i}{\partial t} - e \tilde{\phi} \frac{\partial \tilde{n}_e}{\partial t} = - \int d\Lambda T_e \tilde{n}_e \mathcal{K}(\tilde{\phi}) - \int d\Lambda T_i \tilde{n}_i \mathcal{K}(\tilde{\phi}_G) \quad (15)$$

$$\frac{\partial U_e}{\partial t} = - \int d\Lambda T_e \tilde{n}_e \mathbf{v}_E \cdot \nabla \log n_e + \int d\Lambda T_e \tilde{n}_e \mathcal{K}(\tilde{\phi}) \quad (16)$$

$$\frac{\partial U_i}{\partial t} = - \int d\Lambda T_i \tilde{n}_i \mathbf{u}_E \cdot \nabla \log n_i + \int d\Lambda T_i \tilde{n}_i \mathcal{K}(\tilde{\phi}_G) \quad (17)$$

From this we can see that, since both polarisation and thermal energy for each species now follow from its density equation, the density and corresponding gyroaveraged potential must appear together under spatial derivatives in all conservative processes in order for the energetics to remain consistent. For the ions this is $\tilde{\phi}_G + (T_i/n_i e) \tilde{n}_i$, while for the electrons it is $\tilde{\phi} - (T_e/n_e e) \tilde{n}_e$. Thus, for the ions, the combination $\tilde{\phi}_G + (T_i/n_i e) \tilde{n}_i$ multiplied by the curvature term in Eq. (10) yields a term which vanishes under the integration, conserving the free energy, and the same occurs for the electrons upon multiplying the curvature term in Eq. (9) by $\tilde{\phi} - (T_e/n_e e) \tilde{n}_e$.

This is relatively trivial for such a one-moment gyrofluid model, but the central point is clear: the gyrofluid closure arising from gyroaveraging must be done the same way in the polarisation and in the moment equations. That is, in this case, the operator G in the gyroaveraged potential for a given species must be the same as the one operating upon the corresponding density in the polarisation equation. In a model which incorporates the temperatures, this extends to another gyroaveraging operator acting upon the temperature, and the same one acting upon the potential producing extra finite gyroradius advection terms, plus corrections to the temperature wherever the latter appears under parallel gradients or curvature terms. This is much more involved and will be treated in the next two sections, one discussing the problems with the currently standard gyrofluid model, and the next one formulating the GEM model. Then, the last section shows the applications of GEM to the damping of kinetic shear Alfvén waves, to the hyperfine electron gyroradius scale turbulence problem, and to the Cyclone Base Case which provides the standard benchmark.

II. DRIFT ORDERING AND NORMALISATION CONVENTIONS

With many constant factors containing the physical units to be carried about while manipulating the equations, it is convenient to go to a system of normalised units. While this is somewhat arbitrary, two examples are useful in elucidating the salient units for gyrofluid turbulence. One of these is the prospect of force balance in the electrons along the magnetic field. There are several effects which affect the evolution of the electric current in the electron Ohm's law, but these all act to mediate the response of the electrons to the two static parallel forces: the pressure gradient and the static part of the parallel electric field, given by

$$n_e e \nabla_{\parallel} \phi - \nabla_{\parallel} p_e = p_e \left(\frac{e \nabla_{\parallel} \phi}{T_e} - \nabla_{\parallel} \log p_e \right) \quad (18)$$

assuming small disturbances from the equilibrium, and a field line geometry in which the parallel gradient for finite sized disturbances is not allowed to vanish (see below), a quasistatic balance between these two forces yields the following relationship between the disturbances:

$$\frac{e \tilde{\phi}}{T_e} = \frac{\tilde{p}_e}{p_e} \quad (19)$$

If the parallel responses also equalises the temperature along the field lines, we then have the combination

$$\frac{e \tilde{\phi}}{T_e} = \frac{\tilde{n}_e}{n_e} \quad \frac{\tilde{T}_e}{T_e} = 0 \quad (20)$$

This situation is called adiabatic electrons, and the response to the force in Eq. (18) is called the adiabatic response. The importance of the pressure force is what departs gradient driven turbulence in general from the world of MHD. The adiabatic response indicates the useful units for the electrostatic potential and all the thermodynamic state variables, which will be scaled in terms of T_e/e , n_e , or T_e following the forms in Eq. (20).

The other useful example is closer to the idea of the gyrofluid formulation: the relationship between ion inertia and polarisation. In the low- k_{\perp} limit, the ExB energy is the same as the fluid one,

$$U_E = n_i M_i \frac{v_E^2}{2} = \frac{n_i M_i c^2}{2} \frac{c^2}{B^2} |\nabla_{\perp} \tilde{\phi}|^2 \quad (21)$$

given in Eqs. (6,13). The functional derivative of U_E with respect to $\tilde{\phi}$ leads to the polarisation density

$$\Omega = \frac{n_i M_i c^2}{B^2} \nabla_{\perp}^2 \tilde{\phi} \quad (22)$$

given in Eq. (11). Expressing $\tilde{\phi}$ in terms of T_e/e and the densities in terms of $n_e e$, we find

$$\frac{\Omega}{n_e e} = \frac{n_i}{n_e} \rho_s^2 \nabla_{\perp}^2 \frac{e \tilde{\phi}}{T_e} \quad (23)$$

where ρ_s is the drift scale given by

$$\rho_s^2 = \frac{T_e M_i c^2}{e^2 B^2} \quad (24)$$

This is equally well described in terms of the ion gyroradius,

$$\frac{\Omega}{n_e e} = \frac{n_i T_e}{n_e T_i} \rho_i^2 \nabla_{\perp}^2 \frac{e \tilde{\phi}}{T_e} \quad (25)$$

The role of the drift scale remains, however, even if $T_i \rightarrow 0$, because it is a purely inertial phenomenon. With several species present, T_e and ρ_s make good choices for the basis of the normalisation scheme, and we will use them herein.

We work in terms of an arbitrary number of charged fluids, each with a particular background density and temperature, and mass and charge state per particle. In terms of the electron density and temperature, n_e and T_e , the mass of a main ion species M_i , and the unit of charge, e , we have a normalised background charge density

$$a_z = \frac{n_z Z}{n_e} \quad (26)$$

temperature to charge ratio

$$\tau_z = \frac{T_z}{ZT_e} \quad (27)$$

and mass to charge ratio

$$\mu_z = \frac{M_z}{ZM_i} \quad (28)$$

for each species labelled by z . For electrons, these are $a_e = \tau_e = -1$ and $\mu_e = -m_e/M_i$. For each species, the background mass density is given by $a_z\mu_z$, pressure by $a_z\tau_z$, and squared gyroradius by $\rho_z^2 = \mu_z\tau_z$, in units of n_eM_i , $p_e = n_eT_e$, and ρ_s^2 , respectively. In fusion applications the main ion is often considered to be deuterium, and so the latter mass M_D is used for M_i . However, with discharge experiments run at fusion-relevant normalised parameters using several disparate ion types becoming increasingly important [11], it is important not to make this choice automatic.

We work under drift ordering, also called gyrokinetic ordering. There are two basic perpendicular length scales: the drift scale ρ_s and the background profile scale L_\perp . Drift ordering assumes their ratio to be small,

$$\delta = \rho_s/L_\perp \ll 1 \quad (29)$$

where δ is called the drift parameter. It also assumes that the relative amplitude of all the disturbances is small by this same order, for example,

$$\frac{e\tilde{\phi}}{T_e} \sim \frac{\tilde{n}_z}{n_z} \sim \frac{\tilde{T}_z}{T_z} = O(\delta) \quad (30)$$

and similarly for the parallel flux variables (velocities, heat fluxes) in terms of the sound speed c_s given by

$$c_s^2 = T_e/M_i \quad (31)$$

It also takes a ‘‘maximal’’ ordering with respect to perpendicular wavenumbers and the drift scale,

$$k_\perp\rho_s \sim 1 \quad (32)$$

while assuming a flute/drift ordering for the parallel wavenumber,

$$k_\parallel/k_\perp = O(\delta) \quad (33)$$

The significance of these statements taken together is that the dynamics can be very nonlinear, in the sense that $\mathbf{v}_E \cdot \nabla \sim \partial/\partial t$, even though the disturbance amplitude remains small. It therefore follows that all nonlinearities are dropped except for the quadratic ones represented by ExB advection ($\mathbf{v}_E \cdot \nabla$ in a fluid model, additionally all its finite gyroradius relatives in a gyrofluid model) and, in an electromagnetic model, the ‘‘magnetic flutter’’ nonlinearities represented by the contributions due to the magnetic disturbances in the parallel gradient ∇_\parallel . With the flute ordering we assume that the disturbed and undisturbed parallel gradient pieces are of similar size.

An important implication of drift ordering on the treatment of the geometry concerns the divergences of the various perpendicular drift fluxes. The ExB velocity in an inhomogeneous magnetic field has a finite divergence, so that both $\mathbf{v}_E \cdot \nabla n$ and $n\nabla \cdot \mathbf{v}_E$ would enter a fluid model. However, under drift ordering, both the profile and disturbance are advected at the same order by \mathbf{v}_E , while the factor of n multiplying the divergence is treated as a constant parameter. This forces an explicit split between the advection and divergence terms. Due to their various cancellations [12, 13], the diamagnetic fluxes enter only in the divergences, so this splitting concerns solely the ExB velocity in a fluid model, plus the associated finite gyroradius forms in a gyrofluid model. Under drift ordering, then, the advection term appears as a pure Poisson bracket form (between the two perpendicular coordinates in a field aligned treatment, or between all three pairs in general), multiplied by a constant coefficient, and the divergence term appears as a curvature term (through \mathcal{K} , as above), whose properties are that (1) it is a pure divergence, (2) it is a first order differential operator with the linearity property, and (3) all curvature terms are linear in the dependent variables.

The further impact of drift ordering on the treatment of the magnetic geometry is summarised in the statement that if the three coordinates are aligned to the magnetic field such that one of them is parallel (s), one is radial (x , across flux surfaces, down the gradient), and the third (y) has vanishing projections to both the equilibrium magnetic field and the background gradient, then the variation of the geometry is retained only in s . Field aligning means that only one contravariant component of \mathbf{B} is nonvanishing, in this case B^s . These are the basic statements of field

aligned coordinates and magnetic flux tube geometry, as explained elsewhere [14, 15]. The principal consequence is that the perpendicular Laplacian ∇_{\perp}^2 involves only x and y , and the metric coefficients depend only upon s . Note especially that this includes the variation of the field strength B , whose variation along the magnetic field is retained but commutes with ∇_{\perp}^2 (hence, B^2 appears as a coefficient in the normalised gyroradius in all gyroaveraging and gyroscreening operations). Although the equations of the standard gyrofluid model and of GEM are expressed in covariant terms, the flux tube geometry enters when they are discretised in a numerical representation, and their essential coordinate dependence is reflected in the abovementioned split between advection by and divergence of the drift velocity. We will save further comment on this for the sections (below) describing the numerical scheme.

Thermodynamic state variables are normalised in terms of their background quantities, the electrostatic potential in terms of T_e/e , and the parallel magnetic potential in terms of $B_0\rho_s$. Additionally, a factor of δ is folded into all the normalisations, leaving the ExB advective nonlinearities coefficientless. This is expressed as

$$\tilde{\phi} \leftarrow \delta^{-1} \frac{e\tilde{\phi}}{T_e} \quad \tilde{A}_{\parallel} \leftarrow \delta^{-1} \frac{\tilde{A}_{\parallel}}{B_0\rho_s\beta_e} \quad (34)$$

for the potentials, and

$$\tilde{n}_z \leftarrow \delta^{-1} \frac{\tilde{n}_z}{n_z} \quad \tilde{T}_z \leftarrow \delta^{-1} \frac{\tilde{T}_z}{T_z} \quad (35)$$

$$\tilde{u}_{z\parallel} \leftarrow \delta^{-1} \frac{\tilde{u}_{z\parallel}}{c_s} \quad \tilde{q}_{z\parallel} \leftarrow \delta^{-1} \frac{\tilde{q}_{z\parallel}}{n_z T_z c_s} \quad (36)$$

for the state and parallel flux variables respectively, where

$$\beta_e = \frac{4\pi p_e}{B^2} \quad (37)$$

is the electron dynamical beta (this enters through Ampere's law). The density and temperature are therefore treated on an equal footing with respect to their flux variables, the velocity and heat flux, respectively. Additionally, in both GEM and the standard gyrofluid model, parallel and perpendicular temperatures and parallel-parallel and perpendicular heat fluxes are treated separately, leaving a six moment model, for both ions and electrons as previously [16], and for all species herein.

We leave ∇_{\parallel} normalised in terms of L_{\perp} . Hence, the size of the contravariant magnetic unit vector component b^s is comparable to L_{\perp}/qR , where q is the magnetic pitch parameter (toroidal/poloidal magnetic field, contravariant component ratio), R is the toroidal major radius, and $2\pi qR$ gives the connection length along the magnetic field lines. The parameters governing core or edge turbulence result from competition between ExB turbulence and parallel dynamics, and so the scale ratios enter the ion inertia and curvature parameters according to

$$\hat{\epsilon} = \left(\frac{qR}{L_{\perp}} \right)^2 \quad \omega_B = \frac{2L_{\perp}}{R} \quad (38)$$

respectively. These lead to the parameters governing the parallel electron dynamics,

$$\hat{\beta} = \beta_e \hat{\epsilon} \quad \hat{\mu} = \frac{m_e}{M_i} \hat{\epsilon} \quad C = \frac{0.51\nu_e}{c_s/L_{\perp}} \hat{\mu} \quad (39)$$

These are the drift Alfvén parameter, the electron inertia parameter, and the drift wave collisionality parameter, respectively. For core turbulence C and $\hat{\mu}$ are small, and $\hat{\beta}$ can be in the range from small values to several times 0.1 in high performance tokamaks. For edge turbulence C and $\hat{\mu}$ are larger than unity, and the turbulence becomes electromagnetic for $\hat{\beta}$ near or larger than unity. Ideal and resistive ballooning regimes occur when $\hat{\beta}\omega_B > 1$ or $C\omega_B > 1$, respectively. The magnetic shear parameter is \hat{s} , nominally given by $d \log q / d \log r$ where r is the minor radius but generalisable to arbitrary geometry (cf. Ref. [15]). It is usually of order unity. Under the shifted metric fluxtube geometry, \hat{s} enters only through the shifts incurred in the y -coordinate while taking derivatives with respect to s [20]. Further details on the significance of these parameters may be found in Ref. [9].

III. ENERGETIC PROBLEMS WITH THE STANDARD GYROFLUID MODEL

Most of the problems with the standard gyrofluid model [3, 4] arise from the finite Larmor radius (FLR) terms. The closure approximations are done term by term in a reasonable way, but with subtle differences in the polarisation

equation and in the gyrofluid moment variable equations. In the polarisation equation the gyroaveraging of the distribution function is computed from density and temperature moments of a perturbed Maxwellian approximation. In the moment equations the gyroaveraging is done on the potential (concentrating here upon $\tilde{\phi}$), which is subject to derivatives and then to the moment integrals. These two procedures are in general different unless one approaches them simultaneously with energy conservation in mind. For this reason, the result that the model has inconsistencies is not so unreasonable, particularly considering that its motivation starts with linear theory and only secondarily adds the nonlinearities one needs for turbulence. Additional to this is an inconsistency in treating the higher moments which arise from the curvature terms: a perturbed Maxwellian model is used for those terms while the model itself retains the parallel heat flux moments as dynamical variables. These difficulties are treated in turn, with the FLR terms first. The standard gyrofluid model is sufficiently well constructed that these repairs are in the end a minor matter.

There are three gyroaveraging operators used in the model, given by Eqs. (20,26,27) of Ref. [4],

$$\tilde{\phi}_G = \Gamma_0^{1/2} \tilde{\phi} \quad \frac{1}{2} \widehat{\nabla}_\perp^2 \tilde{\phi}_G = b \frac{\partial \Gamma_0^{1/2}}{\partial b} \tilde{\phi} \quad \widehat{\nabla}_\perp^2 \tilde{\phi}_G = b \frac{\partial^2}{\partial b^2} (b \Gamma_0^{1/2}) \tilde{\phi} \quad (40)$$

assuming a field aligned coordinate system and a Fourier representation in the two perpendicular coordinates, such that $b = k_\perp^2 \rho_i^2$ (the model concentrates on a single ion species and leaves the electrons to be adiabatic). We relabel these in terms of Γ_1 , Γ_2 , and Γ_3 , given by

$$\Gamma_1 = \Gamma_0^{1/2} \quad \Gamma_2 = b \frac{\partial \Gamma_1}{\partial b} \quad \Gamma_3 = \frac{b}{2} \frac{\partial^2}{\partial b^2} (b \Gamma_1) \quad (41)$$

and recast the gyroaveraged and FLR corrected potentials as

$$\tilde{\phi}_G = \Gamma_1 \tilde{\phi} \quad \tilde{\Omega}_G = \Gamma_2 \tilde{\phi} \quad \tilde{\tilde{\Omega}}_G = \Gamma_3 \tilde{\phi} \quad (42)$$

for clarity. Note the factor of two inserted into the definition for Γ_3 , so that $\tilde{\Omega}_G$ and $\tilde{\tilde{\Omega}}_G$ both have the same low- k_\perp limit.

The polarisation equation [17] is given by Eqs. (7,48), rewritten as Eq. (93), all from Ref. [4],

$$\tilde{n}_e = \frac{\tilde{n}_i}{1 + b/2} - \frac{(b/2) \tilde{T}_{i\perp}}{(1 + b/2)^2} + \frac{\Gamma_0 - 1}{\tau_i} \tilde{\phi} \quad (43)$$

preserving the normalisation of $\tilde{\phi}$ in terms of T_e , where $\tilde{T}_{i\perp}$ is the perpendicular temperature disturbance defined as the normalised $(v_\perp^2 - 1)$ moment of the perturbed distribution function. Hence three gyroaveraging operators appear in the moment equations, but only two appear in the polarisation. Moreover, the Padé approximate forms are used in the latter but not in the former. Even if this were repaired, using

$$\Gamma_0^{1/2} \rightarrow \frac{1}{1 + b/2} \quad (44)$$

in the gyroaveraging of the potential (cf. Sec. III.C.4 of Ref. [3]), it would be impossible to reconcile the fact that the $\widehat{\nabla}_\perp^2$ operator does not appear in the polarisation equation, which in terms of the gyroaveraging operators reads

$$\tilde{n}_e = \Gamma_1 \tilde{n}_i + \Gamma_2 \tilde{T}_{i\perp} + \frac{\Gamma_0 - 1}{\tau_i} \tilde{\phi} \quad (45)$$

For the purposes of energetic consistency it does not matter how or whether the $\Gamma_0 - 1$ screening term is approximated, only which operators appear in the \tilde{n}_i and \tilde{T}_i terms.

The ExB energy is given by

$$\int d\Lambda \frac{1 - \Gamma_0}{\tau_i} \frac{\tilde{\phi}^2}{2} \quad (46)$$

Using Eq. (45) we may replace this according to

$$\int d\Lambda \left(\frac{1 - \Gamma_0}{\tau_i} \frac{\tilde{\phi}^2}{2} + \frac{\tilde{\phi} \tilde{n}_e}{2} \right) = \int d\Lambda \tilde{\phi} \left(\frac{\Gamma_1 \tilde{n}_i + \Gamma_2 \tilde{T}_{i\perp}}{2} \right) \quad (47)$$

Using the Hermitian property of the gyroaveraging operators and the definitions of the potentials, and placing the electron contribution on the right side, we find

$$\int d\Lambda \frac{1 - \Gamma_0}{\tau_i} \frac{\tilde{\phi}^2}{2} = \int d\Lambda \left(\frac{\tilde{\phi}_G \tilde{n}_i + \tilde{\Omega}_G \tilde{T}_{i\perp}}{2} - \frac{\tilde{\phi} \tilde{n}_e}{2} \right) \quad (48)$$

The drift energy is therefore expressed as a combination of potentials multiplied by thermal state variables.

If the electrons are adiabatic due to fast parallel dynamics on closed flux surfaces, the electron density is itself replaced by the potential according to

$$\tilde{n}_e = \tilde{\phi} - \langle \tilde{\phi} \rangle \quad (49)$$

where the angle brackets denote the flux surface (“zonal”) average. In this case the electron contribution is a sort of field energy which is combined with the proper drift energy to form the potential energy given by

$$\int d\Lambda \tilde{\phi} \left(\frac{\tilde{\phi} - \langle \tilde{\phi} \rangle}{2} + \frac{1 - \Gamma_0}{\tau_i} \frac{\tilde{\phi}}{2} \right) = \int d\Lambda \left(\frac{\tilde{\phi}_G \tilde{n}_i + \tilde{\Omega}_G \tilde{T}_{i\perp}}{2} \right) \quad (50)$$

The flux surface average is subtracted because the adiabatic state arises through the large value of the parallel wavenumber k_{\parallel} combined with the electron thermal velocity, in comparison with the dynamical frequencies, while for the zonal component there is no action by ∇_{\parallel} . The adiabatic electron approximation does not hold in general, but it is assumed in Refs. [3, 4], and keeping it within this Section makes this discussion more transparent.

The thermal free energy is given by the fluid moment variables in quadratic combination. The state variable free energy is given by

$$\int d\Lambda \left(\tau_i \frac{\tilde{n}_i^2 + \tilde{T}_{i\perp}^2 + \tilde{T}_{i\parallel}^2}{2} \right) \quad (51)$$

while the flux variable free energy (the “generalised parallel kinetic energy”) is given by

$$\int d\Lambda \left(\frac{\tilde{u}_{\parallel}^2 + \tilde{q}_{i\perp}^2 + \frac{2}{3} \tilde{q}_{i\parallel}^2}{2} \right) \quad (52)$$

Comparison of all these pieces leads to the conclusion that the combinations $\tau_i \tilde{n}_i + \tilde{\phi}_G$ and $\tau_i \tilde{T}_{i\perp} + \tilde{\Omega}_G$ should appear together under first derivatives in linear terms in the moment equations in order that in combination among all the energy pieces the various terms reduce to terms involving single first derivative operators acting upon combinations of the variables, which have the form of total divergences, either $B\nabla_{\parallel}$ or \mathcal{K} . It is clear that since no operation by the third gyroaverage Γ_3 appears in the polarisation equation with only densities and temperatures kept in the closure for the total space density, there is no place for the third gyroreduced potential $\tilde{\tilde{\Omega}}_G$ in the moment equations. This is the first and most obvious inconsistency of the standard gyrofluid model, and it impacts the parallel dynamics, the curvature terms (quasistatic compressible part of the drift dynamics), and the magnetic pumping process, each of which we presently examine in turn. Finally, the additional inconsistency in the treatment of higher moments in the curvature terms in the equations for $\tilde{q}_{i\parallel}$ and $\tilde{q}_{i\perp}$ is addressed.

We first look at the parallel dynamics. This involves conservative energy transfer in the sound waves and conductive heat fluxes. The simplest case of a sound wave in the absence of any effects due to the potential is of a parallel gradient in the pressure causing a parallel flow, and the corresponding parallel compression of that flow acting to restore the pressure disturbance. The total divergence term expressing energy conservation in such a local model as this one is $B\nabla_{\parallel}(\tilde{p}\tilde{u}_{\parallel}/B)$, up to numerical constant factors dependent on how the temperatures are described. This divergence represents a transport process, in this case advection of thermal energy by \tilde{u}_{\parallel} . When the potential is also involved, charge currents become part of this, but the structure is the same.

In the standard gyrofluid model, the part of the dynamics involving sound waves is

$$\frac{\partial \tilde{n}_i}{\partial t} = -B\nabla_{\parallel} \frac{\tilde{u}_{\parallel}}{B} \quad (53)$$

$$\frac{\partial \tilde{u}_{\parallel}}{\partial t} = -\nabla_{\parallel} \left[\tau_i \left(\tilde{n}_i + \tilde{T}_{i\parallel} \right) + \tilde{\phi}_G \right] \quad (54)$$

$$\frac{1}{2} \frac{\partial \tilde{T}_{i\parallel}}{\partial t} = -B\nabla_{\parallel} \frac{\tilde{u}_{\parallel}}{B} \quad (55)$$

in addition to the polarisation equation. Evolution of the potential energy, the thermal state variable energy, and the thermal flux variable energy pieces involved in this is given by

$$\tilde{\phi}_G \frac{\partial \tilde{n}_i}{\partial t} = -B \nabla_{\parallel} \frac{\tilde{\phi}_G \tilde{u}_{\parallel}}{B} + \tilde{u}_{\parallel} \nabla_{\parallel} \tilde{\phi}_G \quad (56)$$

$$\tilde{u}_{\parallel} \frac{\partial \tilde{u}_{\parallel}}{\partial t} = -\tilde{u}_{\parallel} \nabla_{\parallel} \left[\tau_i \left(\tilde{n}_i + \tilde{T}_{i\parallel} \right) + \tilde{\phi}_G \right] \quad (57)$$

$$\tau_i \tilde{n}_i \frac{\partial \tilde{n}_i}{\partial t} = -B \nabla_{\parallel} \frac{\tau_i \tilde{n}_i \tilde{u}_{\parallel}}{B} + \tilde{u}_{\parallel} \nabla_{\parallel} \tau_i \tilde{n}_i \quad (58)$$

$$\frac{1}{2} \tau_i \tilde{T}_{i\parallel} \frac{\partial \tilde{T}_{i\parallel}}{\partial t} = -B \nabla_{\parallel} \frac{\tau_i \tilde{T}_{i\parallel} \tilde{u}_{\parallel}}{B} + \tilde{u}_{\parallel} \nabla_{\parallel} \tau_i \tilde{T}_{i\parallel} \quad (59)$$

When the pieces are summed, the transfer terms denoted by $\tilde{u}_{\parallel} \nabla_{\parallel}$ cancel, leaving the total transport divergence term denoted by

$$B \nabla_{\parallel} \frac{\left[\tau_i \left(\tilde{n}_i + \tilde{T}_{i\parallel} \right) + \tilde{\phi}_G \right] \tilde{u}_{\parallel}}{B} \quad (60)$$

that is, just the divergence of a transport flux given by the force potential in the equation for \tilde{u}_{\parallel} multiplied by $\tilde{u}_{\parallel} \mathbf{B}/B$. Here we note that $\tilde{T}_{i\perp}$ is not involved, so there is no action by $\tilde{\Omega}_G$. We find by this analysis that the sound wave dynamics is in order and does not require modification. The same conclusion results from examination of the non-closure part of the heat conduction dynamics, for which the equation parts are

$$\frac{1}{2} \frac{\partial \tilde{T}_{i\parallel}}{\partial t} = -B \nabla_{\parallel} \frac{\tilde{q}_{i\parallel}}{B} \quad (61)$$

$$\frac{\partial \tilde{q}_{i\parallel}}{\partial t} = -\frac{3}{2} \nabla_{\parallel} \left[\tau_i \tilde{T}_{i\parallel} \right] \quad (62)$$

and

$$\frac{\partial \tilde{T}_{i\perp}}{\partial t} = -B \nabla_{\parallel} \frac{\tilde{q}_{i\perp}}{B} \quad (63)$$

$$\frac{\partial \tilde{q}_{i\perp}}{\partial t} = -\nabla_{\parallel} \left[\tau_i \tilde{T}_{i\perp} + \tilde{\Omega}_G \right] \quad (64)$$

and the energetics parts are

$$\frac{1}{2} \tau_i \tilde{T}_{i\parallel} \frac{\partial \tilde{T}_{i\parallel}}{\partial t} = -B \nabla_{\parallel} \frac{\tau_i \tilde{T}_{i\parallel} \tilde{q}_{i\parallel}}{B} + \tilde{q}_{i\parallel} \nabla_{\parallel} \left[\tau_i \tilde{T}_{i\parallel} \right] \quad (65)$$

$$\frac{2}{3} \tilde{q}_{i\parallel} \frac{\partial \tilde{q}_{i\parallel}}{\partial t} = -\tilde{q}_{i\parallel} \nabla_{\parallel} \left[\tau_i \tilde{T}_{i\parallel} \right] \quad (66)$$

and

$$\tau_i \tilde{T}_{i\perp} \frac{\partial \tilde{T}_{i\perp}}{\partial t} = -B \nabla_{\parallel} \frac{\left[\tau_i \tilde{T}_{i\perp} + \tilde{\Omega}_G \right] \tilde{q}_{i\perp}}{B} + \tilde{q}_{i\perp} \nabla_{\parallel} \left[\tau_i \tilde{T}_{i\perp} + \tilde{\Omega}_G \right] \quad (67)$$

$$\tilde{q}_{i\perp} \frac{\partial \tilde{q}_{i\perp}}{\partial t} = -\tilde{q}_{i\perp} \nabla_{\parallel} \left[\tau_i \tilde{T}_{i\perp} + \tilde{\Omega}_G \right] \quad (68)$$

Here we note the factor of two difference in the definition of $\tilde{q}_{i\parallel}$ here (conformal with the Braginskii definition [18]) and in the standard model.

There are also magnetic pumping terms in the gyrofluid parallel dynamics, due to the combination of parallel flow and conduction, magnetic moment conservation at the gyrokinetic level, and the parallel gradient in the strength of the magnetic field. Here, the standard model has the terms in the right places except for a single occurrence of the “forbidden” potential $\tilde{\Omega}_G$:

$$\frac{\partial \tilde{u}_{\parallel}}{\partial t} = - \left[\tau_i \left(\tilde{T}_{i\perp} - \tilde{T}_{i\parallel} \right) + \tilde{\Omega}_G \right] \nabla_{\parallel} \log B \quad (69)$$

$$\frac{1}{2} \frac{\partial \tilde{T}_{i\parallel}}{\partial t} = -(\tilde{q}_{i\perp} + \tilde{u}_{\parallel}) \nabla_{\parallel} \log B \quad (70)$$

$$\frac{\partial \tilde{T}_{i\perp}}{\partial t} = (\tilde{q}_{i\perp} + \tilde{u}_{\parallel}) \nabla_{\parallel} \log B \quad (71)$$

$$\frac{\partial \tilde{q}_{i\perp}}{\partial t} = - \left[\tau_i (\tilde{T}_{i\perp} - \tilde{T}_{i\parallel}) + 2\tilde{\Omega}_G - \tilde{\Omega}_G \right] \nabla_{\parallel} \log B \quad (72)$$

If we merely replace $\tilde{\tilde{\Omega}}_G$ by $\tilde{\Omega}_G$ we restore consistency,

$$\frac{\partial \tilde{q}_{i\perp}}{\partial t} = - \left[\tau_i (\tilde{T}_{i\perp} - \tilde{T}_{i\parallel}) + \tilde{\Omega}_G \right] \nabla_{\parallel} \log B \quad (73)$$

When the free energy pieces are constructed, these effects form transfer channels which then properly conserve energy because $\tau_i \tilde{T}_{i\perp}$ and $\tilde{\Omega}_G$ occur in combination. The reason $\tilde{\tilde{\Omega}}_G$ is “forbidden” is that it doesn’t appear in the polarisation equation. If it is present, then the conservation in the exchange between potential and thermal energy is broken.

A similar problem appears in the curvature terms. For the thermal state variables in the standard model, these are

$$\frac{\partial \tilde{n}_i}{\partial t} = \mathcal{K} \left(\tilde{\phi}_G + \frac{\tilde{\Omega}_G}{2} + \tau_i \frac{\tilde{p}_{i\parallel} + \tilde{p}_{i\perp}}{2} \right) \quad (74)$$

$$\frac{1}{2} \frac{\partial \tilde{T}_{i\parallel}}{\partial t} = \mathcal{K} \left(\frac{\tilde{\phi}_G + \tau_i \tilde{p}_{i\parallel}}{2} + \tau_i \tilde{T}_{i\parallel} \right) \quad (75)$$

$$\frac{\partial \tilde{T}_{i\perp}}{\partial t} = \mathcal{K} \left(\frac{\tilde{\phi}_G + \tilde{\Omega}_G + \tau_i \tilde{p}_{i\perp}}{2} + \frac{3\tau_i \tilde{T}_{i\perp} + \tilde{\Omega}_G + 2\tilde{\tilde{\Omega}}_G}{2} \right) \quad (76)$$

Again, we need merely replace $\tilde{\tilde{\Omega}}_G$ by $\tilde{\Omega}_G$ to restore consistency,

$$\frac{\partial \tilde{T}_{i\perp}}{\partial t} = \mathcal{K} \left(\frac{\tilde{\phi}_G + \tilde{\Omega}_G + \tau_i \tilde{p}_{i\perp}}{2} + 3 \frac{\tau_i \tilde{T}_{i\perp} + \tilde{\Omega}_G}{2} \right) \quad (77)$$

so that $\tau_i \tilde{T}_{i\perp}$ and $\tilde{\Omega}_G$ again occur in combination. Once more, thermal free energy was already conserved in the standard model, but due to $\tilde{\tilde{\Omega}}_G$ a mismatch in the FLR part of the transfer between potential energy and thermal free energy remained.

The curvature terms in the fluid moment flux variables present a different problem, the only inconsistency in the standard model which is not a FLR effect. There are no curvature terms involving the potential in the equations for \tilde{u}_{\parallel} , $\tilde{q}_{i\parallel}$, and $\tilde{q}_{i\perp}$, but there is a closure treatment at the level of the fifth moments which appears in the equations for the third moments ($\tilde{q}_{i\parallel}$ and $\tilde{q}_{i\perp}$), arising from the factors of v_{\perp}^2 and v_{\parallel}^2 in the grad-B and curvature drift terms in the gyrokinetic equation. In the standard model the closure for the 4th and 5th moments is taken from a perturbed Maxwellian (cf. its Eqs. 81 and 82). However, the model retains $\tilde{q}_{i\parallel}$ and $\tilde{q}_{i\perp}$ as dynamical variables, and so the 5th moment should include contributions from pressures times conductive heat fluxes. For example, parts of the $v_{\perp}^2 v_{\parallel}^3$ moment is provided under drift ordering by $p_{i\perp} \tilde{q}_{i\parallel}$ and $p_{i\parallel} \tilde{q}_{i\perp}$, and part of the $v_{\perp}^4 v_{\parallel}$ moment is provided by $p_{i\perp} \tilde{q}_{i\perp}$. In the normalisation, the factors of $p_{i\parallel}$ and $p_{i\perp}$ are replaced by unity. A way to do this systematically is to express the perturbed distribution function as a general six-term polynomial in which each of the coefficients is represented by one of the fluid moment variables retained in the six-moment model. Then, the fifth moments are computed by evaluating the integrals over $v_{\perp}^2 v_{\parallel}$ or v_{\parallel}^3 times the perturbed distribution function. The result of this calculation is a combination which automatically conserves free energy within the fluid moment system:

$$\frac{\partial \tilde{u}_{\parallel}}{\partial t} = \frac{\tau_i}{2} \mathcal{K} (4\tilde{u}_{\parallel} + 2\tilde{q}_{i\parallel} + \tilde{q}_{i\perp}) \quad (78)$$

$$\frac{\partial \tilde{q}_{i\parallel}}{\partial t} = \frac{\tau_i}{2} \mathcal{K} (3\tilde{u}_{\parallel} + 8\tilde{q}_{i\parallel}) \quad (79)$$

$$\frac{\partial \tilde{q}_{i\perp}}{\partial t} = \frac{\tau_i}{2} \mathcal{K} (\tilde{u}_{\parallel} + 6\tilde{q}_{i\perp}) \quad (80)$$

The “diagonal” terms in the implied curvature matrix conserve automatically, but what this procedure has done is to ensure that the “cross” terms also act conservatively.

The final consideration is the ExB advection terms, especially their FLR generalisations. All three potentials ($\tilde{\phi}_G$, $\tilde{\Omega}_G$, and $\tilde{\tilde{\Omega}}_G$) are involved in the standard model, acting through their respective drift velocities,

$$\mathbf{u}_E = -\hat{\mathbf{F}} \cdot \nabla \tilde{\phi}_G \quad \mathbf{w}_E = -\hat{\mathbf{F}} \cdot \nabla \tilde{\Omega}_G \quad \mathbf{W}_E = -\hat{\mathbf{F}} \cdot \nabla \tilde{\tilde{\Omega}}_G \quad (81)$$

where the tensor operator $-\hat{\mathbf{F}} \cdot \nabla$ represents the more familiar $(c/B^2)\mathbf{B} \times \nabla$. The standard model has “diagonal” terms, in which each variable is acted upon by $\mathbf{u}_E \cdot \nabla$ in its own equation, “cross” terms in which the pairs $(\tilde{n}_i, \tilde{T}_{i\perp})$ and $(\tilde{u}_{\parallel}, \tilde{q}_{i\perp})$ are coupled by $\mathbf{w}_E \cdot \nabla$, and then extra “diagonal” FLR effects in which $\tilde{T}_{i\perp}$ and $\tilde{q}_{i\perp}$ are acted upon by $2\mathbf{W}_E \cdot \nabla$ in their own equations. Because $\tilde{\tilde{\Omega}}_G$ is not $\tilde{\Omega}_G$, the FLR potential energy $\tilde{\tilde{\Omega}}_G \tilde{T}_{i\perp} / 2$ is not conserved by $\mathbf{W}_E \cdot \nabla \tilde{T}_{i\perp}$. Again, this is repaired by simply replacing $\tilde{\tilde{\Omega}}_G$ by $\tilde{\Omega}_G$.

Two minor considerations remain: first, the part of the collision process which enforces isotropisation should have the collision frequency multiplying $\tilde{T}_{i\perp} + \tilde{\Omega}_G - \tilde{T}_{i\parallel}$ rather than simply $\tilde{T}_{i\perp} - \tilde{T}_{i\parallel}$, so that the total dissipation is positive definite. This merely captures the correspondence between a gyrofluid $\tilde{T}_{i\perp} + \tilde{\Omega}_G$ and a fluid $T_{i\perp}$ as discussed by Belova [19]. Second, we have discussed energetics independently of nondissipative closure. The standard model constructs a curvature dissipation matrix in order to capture toroidal drift phase mixing by the velocity-dependent grad-B and curvature drifts. Part of this is nondissipative and can in principle capture the 5th moment effects discussed above. However, we choose here to separate these effects because in some applications involving nonperiodic drifts there should be no phase mixing effect at all. Moreover, the dissipation matrix treatment itself is not a real success. It is explained (pp. 4057-8 of Ref. [4]) that a different set of coefficients was required to accurately represent the kinetic result close to marginal stability for the adiabatic-electron, toroidal ITG mode. This is in itself an admission of failure for the project of using the gyrofluid system as a quantitatively exact representation of the gyrokinetic one. We do not attempt such an ambitious goal here; rather, the GEM model is intended for qualitative study of basic physics mechanisms, especially energy transfer between small scale turbulence and large scale flows and MHD processes. Hence the neglect of dissipation free closure effects, and in general the neglect of dissipative effects other than collisions and Landau damping.

The main point of this Section has been to highlight the way in which potential energy and thermal free energy are conservatively exchanged by the various mechanisms involved in low frequency fluid drift dynamics and their capture by a gyrofluid model which is at least well behaved to arbitrary order in the finite Larmor radius parameter $k_{\perp} \rho_i$. If a turbulence model is to act at arbitrary FLR order it should conserve energy properly, even if for no other reason than that a numerical computation should not experience trouble in the spectral region around $k_{\perp} \rho_i \sim 1$. The procedure to repair the standard model accordingly is to restore the use of the same closure treatment (and to the same depth in the number of moments kept) in the polarisation equation(s) and in the fluid moment equations. In the end, the same gyroaveraging operators appear in the polarisation and fluid moment equations — since the polarisation equation in the six-moment model only involves \tilde{n}_i and $\tilde{T}_{i\perp}$ it only involves the first two operators Γ_1 and Γ_2 , and hence only two potentials (one nominal, $\tilde{\phi}_G$, and one FLR, $\tilde{\Omega}_G$) can appear in the fluid moment equations. The third gyroaverage operator Γ_3 may have a reasonable role in a gyrofluid model which retains 4th and 5th moments (one level in the hierarchy past temperatures and conductive heat fluxes), but we do not pursue this extension herein.

IV. CONSTRUCTION OF THE GEM MODEL

Subject to the conventions in Section II, our starting point is the polarisation equation, which links the variables \tilde{n}_z and $\tilde{T}_{z\perp}$ for each species to the electrostatic potential, $\tilde{\phi}$. We neglect true space charge effects, setting the Debye length to zero and assuming the space charge densities all add up to zero. This is the statement of quasineutrality:

$$\sum_z a_z \left[\Gamma_1 \tilde{n}_z + \Gamma_2 \tilde{T}_{z\perp} + \frac{\Gamma_0 - 1}{\tau_z} \tilde{\phi} \right] = 0 \quad (82)$$

where the gyroaveraging and screening operators are defined separately for each species,

$$\Gamma_0 = \Gamma_0(b_z) \quad \Gamma_1 = \Gamma_0^{1/2}(b_z) \quad \Gamma_2 = b_z \frac{\partial \Gamma_1}{\partial b}(b_z) \quad (83)$$

with argument $b_z = k_{\perp}^2 \rho_z^2$ and squared gyroradius $\rho_z^2 = \mu_z \tau_z / B^2$, where B is the normalised strength of the equilibrium magnetic field. The considerations which lead to these forms are the ones given in the standard gyrofluid model [3], as outlined in Section III.

We identify the generalised ExB energy using the polarisation densities in Eq. 82 as

$$U_E = \sum_z a_z \frac{\Gamma_0 - 1}{\tau_z} \frac{\tilde{\phi}^2}{2} \quad (84)$$

Using Eq. 82 and the Hermitian property of the Γ operators, we recast this as

$$U_E = \sum_z a_z \frac{\tilde{\phi}_G \tilde{n}_z + \tilde{\Omega}_G \tilde{T}_{z\perp}}{2} \quad (85)$$

where the gyroreduced potentials are given by

$$\tilde{\phi}_G = \Gamma_1 \tilde{\phi} \quad \tilde{\Omega}_G = \Gamma_2 \tilde{\phi} \quad (86)$$

Note that these are defined separately for each species and that there is no Γ_3 .

We identify the thermal state variable part of the energy the same way as in the fluid models,

$$U_t = \sum_z a_z \tau_z \frac{\tilde{n}_z^2 + (1/2)\tilde{T}_{z\parallel}^2 + \tilde{T}_{z\perp}^2}{2} \quad (87)$$

The flux variable part of the energy is

$$U_v = \sum_z a_z \mu_z \frac{\tilde{u}_{z\parallel}^2 + (2/3)\tilde{q}_{z\parallel}^2 + \tilde{q}_{z\perp}^2}{2} \quad (88)$$

We note here that since the evolution of U_t and U_E ultimately follows from the same moment equations, the combinations which must appear together under the ∇_{\parallel} and \mathcal{K} operators in those equations are $\tilde{\phi}_G + \tau_z \tilde{n}_z$ and $\tilde{\Omega}_G + \tau_z \tilde{T}_{z\perp}$. Observing this will guarantee energetic consistency.

The magnetic field disturbances arise from the parallel magnetic potential, which is given by Ampere's law in terms of the total electric current,

$$-\nabla_{\perp}^2 \tilde{A}_{\parallel} = \tilde{J}_{\parallel} = \sum_z a_z \tilde{u}_{z\parallel} \quad (89)$$

The magnetic energy is given by

$$U_m = \frac{\beta_e}{2} \left| \nabla_{\perp} \tilde{A}_{\parallel} \right|^2 \quad (90)$$

which using Eq. (89) may be rewritten as

$$U_m = \beta_e \frac{\tilde{A}_{\parallel} \tilde{J}_{\parallel}}{2} \quad (91)$$

This model neglects gyroaveraging and gyroscreening of the magnetic potential. On the same footing as the potential equation we would have a more general Ampere's law in which $\tilde{u}_{z\parallel}$ might be replaced by $\Gamma_1 \tilde{u}_{z\parallel} + \Gamma_2 \tilde{q}_{z\perp}$, and due to the same consistency considerations as with $\tilde{\phi}_G$ and $\tilde{\Omega}_G$ several new finite gyroradius terms would appear in the magnetic flutter dynamics. This is being left for future work, however, because the consequences for energy conservation have not yet been worked out.

In situations wherein the finite electron gyroradius is neglected, we simply have $\tilde{\phi}_G = \tilde{\phi}$ and $\tilde{\Omega}_G = 0$ for the electrons, so that the polarisation equation becomes

$$\sum_i a_i \left[\Gamma_1 \tilde{n}_i + \Gamma_2 \tilde{T}_{i\perp} + \frac{\Gamma_0 - 1}{\tau_i} \tilde{\phi} \right] = \tilde{n}_e \quad (92)$$

where the species label is changed to i as it refers to the ions only. If as in most practical applications one takes a single component plasma with singly charged ions, we merely have $a_i = 1$ and $\tau_i = T_i/T_e$, and with normalisation to that particular ion's mass, $\mu_i = 1$ and $\mu_e = -m_e/M_i$ along with $a_e = \tau_e = -1$. Since these are trivial restrictions, we present the GEM model in terms of the general forms following from Eq. (82).

The ExB advection operators and the nonlinear part of the parallel gradient are given in terms of Poisson bracket structures,

$$\mathbf{u}_E \cdot \nabla = [\tilde{\phi}_G,] \quad \mathbf{w}_E \cdot \nabla = [\tilde{\Omega}_G,] \quad \mathbf{b}_\perp \cdot \nabla = -\beta_e [\tilde{A}_\parallel,] \quad (93)$$

in the two perpendicular coordinates, that is,

$$[f, g] = \left(\frac{\partial f}{\partial x} \frac{\partial g}{\partial y} - \frac{\partial g}{\partial x} \frac{\partial f}{\partial y} \right) \quad (94)$$

Defined in this fashion, the quantities \mathbf{u}_E , \mathbf{w}_E , and \mathbf{b}_\perp are all divergence free as written; the generally finite divergences of \mathbf{u}_E and \mathbf{w}_E are treated separately, through $\mathcal{K}(\tilde{\phi}_G)$ and $\mathcal{K}(\tilde{\Omega}_G)$, respectively. The advective time derivative and the parallel derivative are given by

$$\frac{d}{dt} = \frac{\partial}{\partial t} + \mathbf{u}_E \cdot \nabla \quad \nabla_\parallel = \frac{1}{B} \mathbf{B} \cdot \nabla + \mathbf{b}_\perp \cdot \nabla \quad (95)$$

where \mathbf{B} and B are defined in terms of the equilibrium magnetic field. The variation of B along a field line (poloidally around the flux surface in a tokamak) is incorporated into the gyroradii

$$\rho_z^2 = \frac{\mu_z \tau_z}{B^2} \quad (96)$$

The perpendicular parts of the Laplacian are given by

$$\nabla_\perp^2 = \frac{1}{g^{1/2}} \frac{\partial}{\partial x^\mu} g^{1/2} g_\perp^{\mu\nu} \frac{\partial}{\partial x^\nu} \quad (97)$$

where g is the determinant of the $\{g_{\mu\nu}\}$ elements of the entire metric, and $g_\perp^{\mu\nu}$ is the perpendicular metric which involves only the two perpendicular coordinates (x and y). In these terms, the argument b_z appearing in the Γ operators is given by

$$b_z = \rho_z^2 (k_\mu g_\perp^{\mu\nu} k_\nu) \quad (98)$$

where μ and ν are summed over the two perpendicular coordinates only. Note that ρ_z^2 commutes with ∇_\perp^2 and that no gyroradius appears with the ∇_\perp^2 operator in the Ampere's law (Eq. 89).

The six moment equations are the same ones appearing in the toroidal version of the standard gyrofluid model [4], corrected according to the findings in Section III. With \tilde{n}_z and $\tilde{\phi}_G$, and $\tilde{T}_{z\perp}$ and $\tilde{\Omega}_G$, appearing together, and the background gradient forcing terms n_z and T_z (functions of x only) displayed explicitly, the dissipation free part of the equations for each species are

$$\frac{d[n_z + \tilde{n}_z]}{dt} + \mathbf{w}_E \cdot \nabla [T_z + \tilde{T}_{z\perp}] + B \nabla_{\parallel} \frac{\tilde{u}_{z\parallel}}{B} = \mathcal{K} \left(\tilde{\phi}_G + \frac{\tau_z \tilde{p}_{z\parallel} + \tau_z \tilde{p}_{z\perp} + \tilde{\Omega}_G}{2} \right) \quad (99)$$

$$\begin{aligned} \beta_e \frac{\partial \tilde{A}_{\parallel}}{\partial t} + \mu_z \frac{d\tilde{u}_{z\parallel}}{dt} + \mu_z \mathbf{w}_E \cdot \nabla \tilde{q}_{z\perp} &= -\nabla_{\parallel} \left(\tilde{\phi}_G + \tau_z [p_z + \tilde{p}_{z\parallel}] \right) \\ &+ \mathcal{K} \left(\mu_z \tau_z \frac{4\tilde{u}_{z\parallel} + 2\tilde{q}_{z\parallel} + \tilde{q}_{z\perp}}{2} \right) - \tau_z \left(\tilde{\Omega}_G + \tau_z \tilde{T}_{z\perp} - \tau_z \tilde{T}_{z\parallel} \right) \nabla_{\parallel} \log B \end{aligned} \quad (100)$$

$$\begin{aligned} \frac{1}{2} \frac{d[T_z + \tilde{T}_{z\parallel}]}{dt} + B \nabla_{\parallel} \frac{\tilde{u}_{z\parallel} + \tilde{q}_{z\parallel}}{B} \\ = \mathcal{K} \left(\frac{\tilde{\phi}_G + \tau_z \tilde{p}_{z\parallel}}{2} + \tau_z \tilde{T}_{z\parallel} \right) - (\tilde{u}_{z\parallel} + \tilde{q}_{z\parallel}) \nabla_{\parallel} \log B \end{aligned} \quad (101)$$

$$\begin{aligned} \frac{d[T_z + \tilde{T}_{z\perp}]}{dt} + \mathbf{w}_E \cdot \nabla ([n_z + \tilde{n}_z] + 2[T_z + \tilde{T}_{z\perp}]) + B \nabla_{\parallel} \frac{\tilde{q}_{z\perp}}{B} \\ = \mathcal{K} \left(\frac{\tilde{\phi}_G + \tilde{\Omega}_G + \tau_z \tilde{p}_{z\perp}}{2} + 3 \frac{\tilde{\Omega}_G + \tau_z \tilde{T}_{z\perp}}{2} \right) + (\tilde{u}_{z\parallel} + \tilde{q}_{z\perp}) \nabla_{\parallel} \log B \end{aligned} \quad (102)$$

$$\mu_z \frac{d\tilde{q}_{z\parallel}}{dt} = -\frac{3}{2} \nabla_{\parallel} \left(\tau_z [T_z + \tilde{T}_{z\parallel}] \right) + \mathcal{K} \left(\mu_z \tau_z \frac{3\tilde{u}_{z\parallel} + 8\tilde{q}_{z\parallel}}{2} \right) \quad (103)$$

$$\begin{aligned} \mu_z \frac{d\tilde{q}_{z\perp}}{dt} + \mu_z \mathbf{w}_E \cdot \nabla (\tilde{u}_{z\parallel} + 2\tilde{q}_{z\perp}) &= -\nabla_{\parallel} \left(\tilde{\Omega}_G + \tau_z [T_z + \tilde{T}_{z\perp}] \right) \\ &+ \mathcal{K} \left(\mu_z \tau_z \frac{\tilde{u}_{z\parallel} + 6\tilde{q}_{z\perp}}{2} \right) - \tau_z \left(\tilde{\Omega}_G + \tau_z \tilde{T}_{z\perp} - \tau_z \tilde{T}_{z\parallel} \right) \nabla_{\parallel} \log B \end{aligned} \quad (104)$$

The pressures are defined as

$$\tilde{p}_{z\parallel} = \tilde{n}_z + \tilde{T}_{z\parallel} \quad \tilde{p}_{z\perp} = \tilde{n}_z + \tilde{T}_{z\perp} \quad p_z = n_z + T_z \quad (105)$$

and all the thermal state variables are operated upon by $\mathbf{u}_E \cdot \nabla$, $\mathbf{w}_E \cdot \nabla$, and ∇_{\parallel} together with their gradients.

A. Local and Global Models

The GEM model is variously cast in both local and global versions. In the local version the gradient drive terms appear explicitly in the equations as displayed above. Following the ordering, the pressures add linearly also in these quantities. The densities and temperatures are given prescribed forms, usually simple linear gradients, e.g., $n_z = -\omega_n x$ such that $\omega_n = |L_\perp \nabla \log n_z|$ gives the inverse of the normalised scale length, but they can be given arbitrary form, allowing computations within any prescribed gradients. For this version all dependent variables are given Dirichlet boundary conditions in the x -direction,

$$f = 0 \quad \text{at} \quad x = \pm \frac{L_x}{2} \quad (106)$$

where L_x is the domain length.

In the global version the separate gradient terms do not appear in the moment equations. Instead, the fluctuating gradient is part of the dependent variable. Accordingly, the dependent variables are given Neumann/Dirichlet boundary conditions in the x -direction,

$$\frac{\partial f}{\partial x} = 0 \quad \text{at} \quad x = -\frac{L_x}{2} \quad f = 0 \quad \text{at} \quad x = \frac{L_x}{2} \quad (107)$$

allowing arbitrary profile evolution. In this version the curvature operator and also all the dissipation operators act upon the entire variable, including the profile. Consequently, the two dimensional equilibrium including parallel flows and currents, and heat fluxes, is also solved for and evolved self consistently with the turbulence. The transport problem is also solved. One usually operates in one of two limits: the run time is either longer or much shorter than the confinement time. In the latter case sources are not necessary; the profile is allowed to relax but is expected not to do so very much (perhaps 30% relaxation is acceptable). For edge turbulence in a thin radial layer such that $L_x < L_\perp$, the confinement time is usually shorter than the time for the zonal flows, resulting from the evolving flux surface (“zonal”) averaged potential, to reach statistical equilibrium. In this case sources are necessary for all the state variables (\tilde{n}_z and $\tilde{T}_{z\parallel}$ and $\tilde{T}_{z\perp}$ for each species). In either global case, the profiles cannot be prescribed except for the fact that the system is initialised with the profiles set into the state variables.

A final consideration in the global model is polarisation: vorticity is given in general by the “gyrocenter charge density” made up by $\sum_z a_z \tilde{n}_z$, noting that it is the total charge density that is set to zero. Here, the profiles are included in the dependent variables, so especially in the adiabatic electron version one must keep the unchanging $\langle \tilde{n}_e \rangle$ in polarisation,

$$\tilde{n}_e = \langle \tilde{n}_e \rangle + \tilde{\phi} - \langle \tilde{\phi} \rangle \quad (108)$$

where the angle brackets denote the zonal average. In the local version, the profile function $n_i(x)$ does not appear in polarisation, since it is expected to be equal to $n_e(x)$.

Both global and local versions are set up with globally consistent boundary conditions parallel to the background magnetic field. This ensures individual fulfillment of the periodicity constraint for each Fourier component in y as if on the entire flux surface, even if the toroidal mode spectrum is truncated [15]. Here we note that k_y follows the toroidal mode number generally and hence the y -domain is periodic. The domain length for y is L_y . The periodicity constraint applies as a boundary condition in s after one single poloidal cycle, so the s -domain is always one connection length $-\pi < s < \pi$. Additionally, the y -coordinate is shifted on each drift plane (constant- s surface), so that perpendicular dynamics is always computed with an orthogonal metric, and magnetic shear enters as a set of relative shifts in the y -coordinate in the expressions for $\partial/\partial s$, as explained in Ref. [20]. This combination is required for capture of slab-character modes, of which the most important in turbulence is the nonlinear drift wave instability [7, 9, 21]. Global consistency is also required to obtain the correct spectrum of sideband modes in the equilibrium, to which the turbulence and zonal flows are coupled by toroidal compression of the ExB velocity [22].

B. Fourier and Padé Versions

The operators involving ∇_\perp^2 , including the Γ 's, are solved variously in xy -space or in \mathbf{k}_\perp -space. The Fourier versions are set up to be compatible with either the local or global boundary conditions. The local model with Dirichlet boundaries uses half-wave Fourier transforms, with the basic x -domain odd-reflected about $x = L_x/2$, that is, $f(L_x/2 + x') = -f(L_x/2 - x')$ for $0 < x' < L_x$. The Fourier transform and its inverse is then applied to the doubled domain. In a similar manner, the global model uses quarter-wave Fourier transforms, with four copies of

the x -domain arrayed odd-even-even-odd, and with the transforms applied to the quadrupled domain. This Fourier version of either the local or global model is used whenever the argument $b_z = k_\perp^2 \rho_z^2$ of any species is expected to take large values. The hallmark example of this is ETG turbulence (Sec. V), which involves the entire scale range between ρ_i and ρ_e in a single component plasma. If the ion moment variables are kept, the Fourier version should be used to obtain an accurate ion response, which becomes more and more “adiabatic” (in the sense that $\tilde{\phi} \rightarrow -\tau_i \tilde{n}_e$) with increasing b_i . In current implementations, the Fourier version always uses the full FLR form for every species, including electrons, regardless of the expected values of b_z .

For standard ITG or edge turbulence cases, where the scale range reaches down to but not below ρ_i , the Padé version may be used. This approximates the Γ ’s by [3]

$$\Gamma_0(b_z) \rightarrow (1 - \rho_z^2 \nabla_\perp^2)^{-1} \quad (109)$$

$$\Gamma_1(b_z) \rightarrow \left(1 - \frac{1}{2} \rho_z^2 \nabla_\perp^2\right)^{-1} \quad (110)$$

$$\Gamma_2(b_z) = \frac{1}{2} \rho_z^2 \nabla_\perp^2 \left(1 - \frac{1}{2} \rho_z^2 \nabla_\perp^2\right)^{-1} \Gamma_1(b_z) \quad (111)$$

However, if the finite gyroradius effects of more than one species are taken into account, one must solve the combined screening operator given by $\sum_z (a_z / \tau_z) (\Gamma_0 - 1)$ to find $\tilde{\phi}$. This is simple in \mathbf{k}_\perp -space but complicated if using the Padé forms in configuration space, even if one of the coordinates is Fourier decomposed. With only two gyroradii to follow, however, one has the acceptable operation involving two successive Helmholtz solves. In current implementations, the Padé version is only used for single component plasma cases in which the electron FLR effects are neglected. The adiabatic ion model is only used with the Padé version. The importance of the Padé version is that it is the only one easily generalised to fully global geometry, wherein the metric coefficients depend on x .

C. Dissipation in GEM – Collisionless

The only true dissipation in the collisionless GEM model is phase mixing due to the kinetic resonances caused by the parallel transit dynamics, i.e., Landau damping. This is represented by direct dissipation upon the parallel heat flux variables, using a Landau damping operator defined by

$$a_{Lz} \equiv a_{L0} \left(1 - 0.125 V q R \nabla_\parallel^2\right) \quad (112)$$

with constant a_{L0} nominally set to unity, where qR is the field line connection length divided by 2π [15], $V = \tau_z / \mu_z$ is the normalised thermal speed of species z , and ∇_\parallel^2 is generally the full nonlinear parallel Laplacian divergence operator $B \nabla_\parallel (1/B) \nabla_\parallel$. Both qR and ∇_\parallel^2 are normalised in terms of L_\perp .

The GEM model does not employ a curvature drift dissipation model. The standard one did so [4], but also noted in detail the problems it raised. For the reasons discussed in Section III, therefore, it is chosen to omit this feature. Nonlinear FLR phase mixing [3] is also left out of the standard model [4], for similar reasons of tractability.

D. Dissipation in GEM – Collisional

The electromagnetic gyrofluid model finds a very useful application in tokamak edge turbulence [16], and hence requires a treatment of collisions which will capture the collisional Braginskii fluid model [18] in the appropriate limit of large collision frequency and short mean free path. The usual types of dissipation are resistivity and thermal conduction, which in a model treating both velocities and heat fluxes as dynamical variables amounts to applying a dissipation matrix to their combination. For an isotropic temperature the method used in the DALF Landau fluid model [8] is sufficient. The gyrofluid model, however, additionally includes temperature anisotropy. To combine these effects, a simple drift kinetic Chapman-Enskog procedure is used to find the dissipative corrections to a state with stationary state variables [23], generalised to a bi-Maxwellian distribution (defined by \tilde{n}_z , $\tilde{T}_{z\parallel}$, and $\tilde{T}_{z\perp}$ for each species) for the dissipation free part. A Lorentz collision operator is used, and then the Braginskii coefficients are substituted to capture the collisional limit. The resulting model is given by

$$\beta_e \frac{\partial \tilde{A}_\parallel}{\partial t} + \mu_z \frac{d \tilde{u}_{z\parallel}}{dt} = \dots + \mu_e \nu_e \left[\eta \tilde{J}_\parallel + \frac{\alpha_e}{\kappa_e} \left(\tilde{q}_{e\parallel} + \tilde{q}_{e\perp} + \alpha_e \tilde{J}_\parallel \right) \right] \quad (113)$$

$$\frac{1}{2} \frac{d\tilde{T}_{z\parallel}}{dt} = \dots - \nu_z \left[\tau_z \left(\tilde{T}_{z\parallel} - \tilde{T}_{z\perp} \right) - \tilde{\Omega}_G \right] \quad (114)$$

$$\frac{d\tilde{T}_{z\perp}}{dt} = \dots + \nu_z \left[\tau_z \left(\tilde{T}_{z\parallel} - \tilde{T}_{z\perp} \right) - \tilde{\Omega}_G \right] \quad (115)$$

$$\mu_z \frac{d\tilde{q}_{z\parallel}}{dt} = \dots - \frac{(5/2)}{\kappa_z} \mu_z \nu_z \left(\tilde{q}_{z\parallel} - 0.6\alpha_z \tilde{J}_{\parallel} \right) + 1.28\nu_z \left(\tilde{q}_{z\parallel} - 1.5\tilde{q}_{z\perp} \right) \quad (116)$$

$$\mu_z \frac{d\tilde{q}_{z\perp}}{dt} = \dots - \frac{(5/2)}{\kappa_z} \mu_z \nu_z \left(\tilde{q}_{z\perp} - 0.4\alpha_z \tilde{J}_{\parallel} \right) - 1.28\nu_z \left(\tilde{q}_{z\parallel} - 1.5\tilde{q}_{z\perp} \right) \quad (117)$$

where κ_z and α_z are the thermal conduction and thermal force coefficients for each species, and η_{\parallel} is the resistivity coefficient. Herein, the thermal force is kept only for electrons ($\alpha_z = \alpha_e$), while for ions it is zero. For a single component plasma with singly charged ions, the values of the coefficients are

$$\eta = 0.51 \quad \alpha_e = 0.71 \quad \kappa_e = 3.2 \quad \kappa_i = 3.9 \quad (118)$$

To recover an isotropic model we would add $(1/2)\tilde{T}_{z\parallel} + \tilde{T}_{z\perp}$ to form $(3/2)\tilde{T}_z$ and $\tilde{q}_{z\parallel} + \tilde{q}_{z\perp}$ to form $\tilde{q}_{z\parallel}$. This yields the forms in Ref. [8]. Then, we could recover the Braginskii formula for $\tilde{q}_{z\parallel}$ by neglecting the inertial and Landau damping terms in its equation (i.e., neglect $\tilde{q}_{z\parallel}$ except in the collisional damping term), as explained in Ref. [8].

The terms in the temperature equations and the ones with the factors of 1.28 represent relaxation of anisotropy, and the others represent resistive (η) and thermal conductive (κ_z) dissipation. Note the combination $\tau_z \tilde{T}_{z\perp} + \tilde{\Omega}_G$ in the temperature equations; this is required to make the dissipation positive definite, following the same considerations as those concerning energy conservation resulting from the same combination under the ∇_{\parallel} and \mathcal{K} operators.

E. Nonlinear Dissipation and the Numerical Scheme in GEM

One final dissipation mechanism remains to be considered, and in gradient driven turbulence it is often the most important one: nonlinear cascading to arbitrarily small scales [21]. This enters explicitly as an artificial diffusion term in each equation for computations using a dissipation free scheme to calculate the nonlinear advection terms.

The energy cascade in drift wave turbulence is generally local in \mathbf{k}_{\perp} -space [24], and can proceed in either direction following the properties of the various nonlinearities [24, 25, 26]. When energy cascades to the scale of the computational grid (highest k_{\perp} values), it must be removed somehow lest the spectra approach the unphysical forms representing the maximum entropy state [25] of the discrete system. One must check to ensure that the grid dissipation rate is independent of the resolution, essentially the same statement contained in high Reynolds number turbulence (dissipation independent of the diffusion or viscosity coefficient).

In the past, the predecessor of this model has used an upwind scheme (a slope limiting algorithm [27] integrating all the dimensions together [28], from computational fluid dynamics) implemented as discussed elsewhere [16]. Herein, we employ an alternative finite difference scheme which also does not involve Fourier transforming or spectral operations and hence is applicable to situations forbidding such operations. The scheme has been used with success by Naulin on the fluid drift Alfvén model [29]. The first derivatives involved in Poisson bracket structures are evaluated with the second-order version of the Arakawa spatial discretisation [30]. The linear terms involving parallel dynamics ($\partial/\partial s$) and perpendicular compressibility (\mathcal{K}) are evaluated with standard second-order central differences. Direct dissipation terms (e.g., collision-based frictional damping of \tilde{J}_{\parallel} or Landau-based damping of heat fluxes) are evaluated directly. The entire right side is evaluated thereby once per time step, but using a third-order “stiffly stable” algorithm derived by Karniadakis *et al.*, according to which the previous three time steps of the dependent variables and the right hand sides are used to get the new time step [31]. Since the entire right hand side is used this way, an unsplit second-order accuracy is achieved. Finally, the artificial dissipation terms are applied separately, using the dependent variables at the now-previous timestep. The structure of the equations is given by

$$\frac{\partial F}{\partial t} = S + D(f) \quad (119)$$

where F is the functional of the dependent variables f appearing under the $(\partial/\partial t)$ operator in each equation, S is the right hand side of each equation, and D is the artificial dissipation operator in each equation. The structure of

the algorithm is given by

$$S_0 = S(f_0) \quad (120)$$

$$F_1 = \frac{6}{11} \left[3F_0 - \frac{3}{2}F_{-1} + \frac{1}{3}F_{-2} + \Delta t (3S_0 - 3S_{-1} + S_{-2}) \right] \quad (121)$$

$$F_1 \leftarrow F_1 + \Delta t D(f_0) \quad (122)$$

$$\text{(apply boundary conditions)} \quad (123)$$

$$f_1 \leftarrow F_1 \quad (124)$$

where the subscript ‘0’ refers to the current timestep, ‘1’ refers to the new timestep, and the negative ones refer to the previous timesteps, Δt is the timestep interval, “boundary conditions” refers to the loading of the guard cells at the computational boundary so that derivatives are computed normally during the evaluations of S and D , and the last step recovering f_1 from F_1 refers to the solving of the polarisation equations to recover $\tilde{\phi}$ and \tilde{A}_{\parallel} and the evaluation of the gyroaveraging operators Γ_1 and Γ_2 to get the gyroreduced potentials $\tilde{\phi}_G$ and $\tilde{\Omega}_G$. For waves, this scheme is stable without the use of D , allaying the principal consideration which led to the upwind scheme in the first place [16]. But for turbulence we require the use of D .

It is important to note that the artificial dissipation must work in all three coordinates, not just the two perpendicular ones. ExB advection is the main agent causing the direct cascade towards large wavenumbers in the gyrofluid state variables, mostly \tilde{n}_z (for edge turbulence) but also $\tilde{T}_{z\parallel}$ and $\tilde{T}_{z\perp}$ (almost solely, for core turbulence). It is important to note that this occurs not only in \mathbf{k}_{\perp} -space but also k_{\parallel} -space, simply due to the statistics [32]. The dissipation operators must therefore function for both k_{\perp}^2 and k_{\parallel}^2 .

One might be tempted to apply D to the force potentials, e.g., $\tilde{n}_z - \tilde{\phi}_G$ instead of \tilde{n}_z , but this has been found to damage the solution measurably. It is indeed important not to apply artificial dissipation directly to either ϕ or \tilde{A}_{\parallel} , the main effect of that being to destroy the Alfvén dynamics (for k_{\parallel}^2) or medium to large scale vorticity (for k_{\perp}^2). This was the problem with the upwind scheme [16]: as the kinetic shear Alfvén velocity is scale dependent the exact one could not be used in the flux splitting involved in the scheme, so the fastest one was used (otherwise, the scheme is unstable). For $\beta_e < m_e/M_i$ the fastest wave (following v_A) is at the lowest k_{\perp} and the smallest scales (highest k_{\perp}) are dominated by collisional dissipation anyway (since $\nu_e > c_s/L_{\perp}$), so edge turbulence was not strongly impacted. For core turbulence, on the other hand, the fastest wave (following V_e) is at the highest k_{\perp} so that the large scale MHD response at the lowest k_{\perp} is strongly dissipated with a sort of super-resistivity acting directly upon \tilde{A}_{\parallel} rather than \tilde{J}_{\parallel} . To avoid the same problem with schemes with explicitly applied artificial dissipation, it is important to avoid application of any of the artificial dissipation operators directly to \tilde{A}_{\parallel} .

In the xy -plane the operations are summarised by the statement

$$\mathbf{u}_E \cdot \nabla \rightarrow \mathbf{u}_E \cdot \nabla - \nu_{\perp} \nabla_{\perp}^2 - \nu_{\parallel} \nabla_{\parallel}^2 \quad (125)$$

in each equation; that is, artificial dissipation in both the xy -plane and the s -direction is applied to whatever is advected by the gyroreduced ExB velocity. An alternative is a hyperdiffusion for the xy -plane, so that

$$\mathbf{u}_E \cdot \nabla \rightarrow \mathbf{u}_E \cdot \nabla + \nabla_{\perp}^2 \nu_{\perp} \nabla_{\perp}^2 - \nu_{\parallel} \nabla_{\parallel}^2 \quad (126)$$

is used. For models with variable B these should be respectively changed to

$$\mathbf{u}_E \cdot \nabla \rightarrow \mathbf{u}_E \cdot \nabla - \nabla \cdot \nu_{\perp} \rho_s^2 \nabla_{\perp} - \nabla \cdot (\mathbf{b} \nu_{\parallel} \mathbf{b}) \cdot \nabla \quad (127)$$

and

$$\mathbf{u}_E \cdot \nabla \rightarrow \mathbf{u}_E \cdot \nabla + \nabla_{\perp}^2 \nu_{\perp} \rho_s^4 \nabla_{\perp}^2 - \nabla \cdot (\mathbf{b} \nu_{\parallel} \mathbf{b}) \cdot \nabla \quad (128)$$

with

$$\rho_s^2 = \frac{1}{B^2} \quad (129)$$

in normalised units, so that the property of positive definiteness is preserved. If variable resolution causes problems, then the metric elements in these forms should be replaced by their flux surface averages.

Typical values of these dissipation coefficients are set depending on the physical situation; in general they must be set as small as possible. Full resolution is found when it can be shown the resulting grid dissipation rate (not

necessarily the answer for the transport fluxes) is independent of the dissipation parameters. A resolution study will generally not be done at a particular value of the coefficient; rather, the coefficient should be made smaller when the resolution is increased. A window of operation opens when it is subsequently found that the above criteria for full resolution is met. Tests on core turbulence with adiabatic electrons ($\nu_e = \beta = \mu_e = 0$) find that ν_\perp as small as 10^{-2} is possible with resolutions of $h_x = h_y = 1$ or $2 \times \rho_s$. Edge turbulence ($C, \hat{\beta}, \hat{\mu}$ all unity or greater; cf. Section II and Ref. [9]) requires $h_x = h_y = 1 \times \rho_s$ or smaller to be able to reduce ν_\perp to as small as 3×10^{-2} . With $h_x = h_y = 2 \times \rho_s$ a value of $\nu_\perp = 0.1$ can be required, and this is generally too large to allow the vorticity dynamics in the range $0.5 < k_\perp \rho_s < 1$ to function properly. This is due to the robust nonlinear action by $\mathbf{v}_E \cdot \nabla \tilde{n}_e$ in edge turbulence [21]. Under these conditions the hyperdiffusion form is necessary to be able to reproduce the nonlinear drift wave instability. For cold ion models ($\tau_i = 0$) with no temperature dynamics, this instability can be reproduced with a resolution of $h_x = h_y = 2$ and a hyperdiffusion of $\nu_\perp = 0.01$.

The parallel dissipation coefficients are easier as they are only needed to contain the cascade in the parallel wavenumber k_\parallel by the nonlinear perpendicular dynamics. Values of $\nu_\parallel = 3 \times 10^{-3}$ for both ions and electrons are found to be sufficient with $h_s = 2\pi qR/16$, and for the most important wavenumber range $-2 < k_\parallel qR < 2$ these lead to small corrections to the physical dissipation rates. It has been found necessary to use the same coefficient for both ions and electrons, to avoid artificial charge separation which can have a large effect on the spectral region with $k_\parallel qR$ moderate and $k_\perp \rho_s$ small.

V. SELECTED COMPUTATIONAL RESULTS

It is not the purpose of this paper to enter detailed study of any of the problems the GEM model is to be applied to; rather, the focus is upon the way energetics works in the model and to use that to assist consistent construction of the model. Nevertheless, it is useful to apply the model briefly herein to an elementary situation whose capture is important (kinetic shear Alfvén wave damping [33, 34]), a well known set of computational results (the Cyclone ITG turbulence campaign [1]), and a demonstration that electron driven turbulence at scales below the ion gyroradius can be addressed with a gyrofluid model (“ETG” [35]). The latter two cases will be treated in proper detail in the future. ETG turbulence has been treated with a fluid model before, but only with adiabatic ion models [36, 37, 38]. Herein, we apply GEM directly and find the ETG dynamics occurring naturally at its native scales.

A. Kinetic shear Alfvén wave damping

Shear Alfvén waves are well known from MHD [39], and the collisionless kinetic counterpart (KALF) is also well known [40]. It has already been shown the gyrokinetic model treats them properly [33, 34]. We now use the result to calibrate the model Landau damping coefficient for the electrons.

We take a basic parameter case with $\hat{\beta} = 1$ and $\hat{\mu} = 1$ and $\hat{\epsilon} = 18350$ with both collisionalities set to zero as a reference. The magnetic field is straight and homogeneous ($g^{xx} = g^{yy} = B = 1$ with $\hat{s} = 0$ and $\mathcal{K} = 0$) and there are no background gradients ($\omega_n = \omega_t = \omega_i = 0$). The ions are cold ($\tau_i = 0$ hence $\rho_i = 0$). The Padé version of the local model is used. With the homogeneous situation, the profile functions are set to zero and the domain is periodic in both y and s . The perpendicular domain sizes are $L_x = L_y = 2\pi/K$, with $K = 0.1$. The parallel domain is one connection length. The initial state is the sinusoidal disturbance $\tilde{n}_e = 10^{-4}(1 + \cos Kx) \cos Ky \cos s$, with $\tilde{n}_i = \tilde{n}_e$. The grid was $32 \times 32 \times 16$ in $\{x, y, s\}$. The values of $\hat{\beta}$ and $\hat{\mu}$, and the Landau damping model coefficient a_{L0} , were varied between 0.1 and 10. Artificial dissipation (ν_\perp and ν_\parallel) was set to zero.

The KALF dispersion relation, shown in Fig. 1, has the two standard asymptotic limits $\hat{\beta}/\hat{\mu} \gg 1$ and $k_\perp^2 \ll 1$ where for these cases $k_\perp^2 = (5/4)K^2$. This range is found with the nominal sweep in $\hat{\beta}$ for $\hat{\beta} \gg 1$, and in the sweep in $\hat{\mu}$ for $\hat{\mu} \ll 1$, and is well captured by the GEM model as shown by the comparison to the kinetic result using the root finding method of Ref. [34]. When $\hat{\beta} \approx \hat{\mu}$ there is substantial thermal electron resonance. In this regime the GEM model shows a peak, but with the peak value and its location only approximately captured. In the sweep of a_{L0} the damping rate was proportional to a_{L0} only for $a_{L0} < 1$. For $a_{L0} > 1$ the effect is to remove the parallel heat flux from the dynamics, which becomes more ideal; hence the damping rate falls again. The maximum is found for $a_{L0} = 1.6$, which is close to the actual thermal resonance at $\sqrt{3}$. The damping rate varies within the interval $8.5 < -10^3 \gamma_L < 9.6$ for $1 < a_{L0} < 2$. As a robust model in the absence of fitting for all possible cases, it appears to be sufficient to simply leave $a_{L0} = 1$, and the model performs qualitatively well.

B. ITG turbulence

The standard of core turbulence studies with adiabatic electrons is the Cyclone project, which benchmarked a series of models and computations against a particular case of hot ion collisionless turbulence and transport [1]. With the only free energy source being the ion temperature gradient, this is called ITG turbulence. With adiabatic electrons taken as a model ($\hat{\beta} = \hat{\mu} = C = 0$), the parameter set is given by

$$\begin{aligned} \omega_B &= 0.290 & \hat{\epsilon} &= 93.4 & \hat{s} &= 0.78 \\ \omega_t = \omega_i = \tau_i &= 1 & \omega_n &= 0.321 \end{aligned} \quad (130)$$

The artificial dissipation coefficients are $\nu_{\perp} = 0.01$, using hyperdiffusion, and $\nu_{\parallel} = 0.001$. The boundary dissipation coefficient was 1.0. For the magnetic field the simple circular tokamak model with globally consistent boundary conditions and shifted metric coordinate system is used as detailed in Ref. [20]. The potential is initialised with a random disturbance bath in x and y [7] and a parallel envelope following the field lines from $s = 0$ [20], and an RMS amplitude of 10^{-8} . The Padé version of the global model is used. The basic profile is given by

$$p_0(x) = \frac{L_x}{2} \left(1 - \sin \frac{\pi x}{L_x} \right) \quad (131)$$

and then both densities are initialised with $\omega_n p_0 + \tilde{\phi}$ and the ion temperatures ($\tilde{T}_{i\parallel}, \tilde{T}_{i\perp}$) with $\omega_i \tau_i p_0$. The adiabatic form of the polarisation equation with profiles is used, with $\langle \tilde{n}_e \rangle = \omega_n p_0(x)$, noting that ω_t has no role for this problem. The perpendicular domain sizes are $L_x = L_y = 80\pi$, roughly commensurate with the global tokamak dimensions of $a/\rho_s = 192$ and $2\pi r/q\rho_s = 350$ (where $r = a/2$). The parallel domain is one connection length. The grid was $128 \times 128 \times 16$ in $\{x, y, s\}$.

The four cases with $\omega_i = \{0.8, 1.0, 1.5, 2.2\}$ were taken. Normalisation of the transport level is to L_n , following Ref. [1], so that the transport flux in units of the nominal L_{\perp} , $Q_i = \left\langle (0.5\tilde{T}_{i\parallel} + \tilde{T}_{i\perp})\tilde{v}_E^x \right\rangle$, is recast in terms of a transport coefficient by taking $\chi_i = Q_i/(\omega_n |\nabla T|)$. Each run begins in a linear growth phase, overshoots to a transport level in the vicinity of $\chi_i = 10$, and then saturates with the zonal flow dynamics (the part of the ExB flow arising from $\langle \tilde{\phi} \rangle$) reaching statistical equilibrium only well after $t = 1000$. Runs were taken to $t = 4000$. The transport is displayed statistically, with a sample taken at intervals of $\Delta t = 10$ in the phase $1000 < t < 4000$. Slow relaxation of the temperature profile fills out the transport scaling curve. For each sample, the flux and gradient were averaged over all grid nodes in the part of the domain with $0 < x < L_x/4$ before their ratio was computed.

The resulting transport curve is shown in Fig. 2, wherein the triangle markers denote each sample (1200 in all), and the dashed curve is the fit to the gyrokinetic particle model results as given in Ref. [1]. Agreement at the 20% level is found for most of the curve, and moreover the nonlinear threshold agrees within the statistical scatter. Moreover, the fact that the groups of points from four decaying runs overlap well indicates the transport to be temporally local.

C. ETG turbulence

A class of turbulent dynamics at scales smaller than ρ_i driven by ∇T_e is called ETG [35]. Neither ∇n nor ∇T_i is available as a drive because the ions are adiabatic (in the simplest treatments) or nearly so. Here, we carry both electrons and ions with the full six moments and allow the spatial scale range kept in the particular case to determine the dynamics. The Fourier version of the local model is used, with profile functions $n_e = n_i = -\omega_n x$ and $T_e = -\omega_t x$ and $T_i = -\omega_i x$. The same magnetic geometry as in the ITG examples above is used. The same random bath as above is used initially, but for \tilde{n}_e .

Here we merely demonstrate the ability of the GEM model to capture this ETG turbulence for typical core parameters, the same as the one used for the ITG examples above, additionally with $\hat{\beta} = 0.464$ and $\hat{\mu} = 0.0254$ and $\nu_e = 0.0333$. The artificial dissipation coefficients were $\nu_{\perp} = 3 \times 10^{-3}$ (using simple diffusion, not hyperdiffusion) and $\nu_{\parallel} = 10^{-4}$. The initial RMS amplitude for \tilde{n}_e was $a_0 = 3 \times 10^{-3}$. The spatial domain size was $L_x = L_y = 4\pi/3$ for the drift plane and one connection length along the magnetic field. The grid was $128 \times 128 \times 16$ in $\{x, y, s\}$. The timestep was 5×10^{-4} . The run was carried for $20L_{\perp}/c_s$. With the minimum value of $k_y \rho_i$ of 1.5, ITG activity is generally absent. The fastest growing spectral range is about $10 < k_y < 20$, representing structure scales $\Delta y = \pi/k_y$ on the order of $10\rho_e$. The spatial morphology shows these to be radially extended, with $\Delta x > 8\Delta y$. The nonlinear transition begins at $t \approx 8$ and saturation occurs after $t \approx 12$. A very strong transport level is found, just under 0.1, which in terms of electron scales is $\chi_e \approx 6\rho_e^2 V_e/L_T$. The spectrum is broader than in the linear phase, but still narrow compared to edge turbulence, and more importantly the transport spectrum peaks at $k_y = 10$, very close to the linear

growth peak. The radially extended structures do persist in the saturated phase, by contrast to typical core ITG or edge turbulence. These features, shown for both linear and nonlinear phases in Fig. 3, are the same as those shown previously by nonlinear gyrokinetic studies [35]. The amplitude of the electron moment variables \tilde{n}_e and $\tilde{T}_{e\parallel}$ is about 0.2, while the corresponding ion variables are about two orders of magnitude smaller.

VI. SUMMARY

The standard local gyrofluid model has been placed on energetically consistent grounds, with the moment variables and the electrostatic potential given a full finite Larmor radius (FLR) treatment at the same level of sophistication. The FLR effects on the magnetic potential and parallel velocities and heat fluxes is left to the future. With these changes it is possible to recover important results emerging from gyrokinetic computations, with a computationally more tractable model. Large systems may be treated with full resolution with what at present time may be regarded as modest computational resources. The model is flexible, to the extent that the level of sophistication can be increased or decreased while retaining energetic and geometric consistency. Both global and local situations can be treated. Highly detailed dissipative linear closures as discussed in the main references [3, 4] are not necessary in many cases of interest, in particular the one from the Cyclone study (Ref. [1]).

For proper edge turbulence ($\hat{\mu} > 1$ and $C > 1$) in the electromagnetic regime ($\hat{\beta} > 1$) the model functions much as in previous versions as published elsewhere [16]. Results from the two moment version GEM3 (density and parallel velocity for both electrons and ions) are published elsewhere [9], showing the role of the three dimensional drift wave nonlinear instability in the context of tokamak edge turbulence as done previously [21] for the corresponding fluid model. Work with cases with various ratios of $\eta_i = \omega_i/\omega_n$ (cf. [21] for the role of this in the fluid model) and with two ion species is in progress.

-
- [1] A. M. Dimits, G. Bateman, M. A. Beer *et al*, Phys. Plasmas 7 (2000) 969.
 - [2] G. Knorr, F. R. Hansen, J. P. Lynov, H. L. Pécseli, and J. Juul Rasmussen, Physica Scripta 38 (1988) 829.
 - [3] W. Dorland and G. Hammett, Phys. Fluids B 5 (1993) 812.
 - [4] M. A. Beer and G. Hammett, Phys. Plasmas 3 (1996) 4046.
 - [5] M. Wakatani and A. Hasegawa, Phys. Fluids 27 (1984) 611.
 - [6] R. E. Waltz, Phys. Fluids B 2 (1990) 2118.
 - [7] B. Scott, Phys. Rev. Lett 65. (1990) 3289; Phys. Fluids B 4 (1992) 2468.
 - [8] B. Scott, Plasma Phys. Contr. Fusion 39 (1997) 1635.
 - [9] B. Scott, Plasma. Phys. Contr. Fusion 45 (2003) A385.
 - [10] P. Rutherford and E. A. Frieman, Phys. Fluids 11 (1968) 569; J. B. Taylor and R. J. Hastie, Plasma Phys. 10 (1968) 479.
 - [11] N. Krause, C. Lechte, J. Stoeber, U. Stroth, E. Ascasibar, J. Alonso, and S. Niedner, Rev. Sci. Instrum. 73 (2002) 3474.
 - [12] S.-T. Tsai, F. W. Perkins, and T. H. Stix, Phys. Fluids 13 (1970) 2108.
 - [13] F. L. Hinton and C. W. Horton, Jr, Phys. Fluids 14 (1971) 116.
 - [14] M. A. Beer, S. C. Cowley, and G. W. Hammett, Phys. Plasmas 2 (1995) 2687.
 - [15] B. Scott, Phys. Plasmas 5 (1998) 2334.
 - [16] B. Scott, Phys. Plasmas 7 (2000) 1845.
 - [17] W. W. Lee, Phys. Fluids 26 (1983) 556.
 - [18] S. I. Braginskii, Rev. Plasma Phys. 1 (1965) 205.
 - [19] E. V. Belova, Phys. Plasmas 8 (2001) 3936.
 - [20] B. Scott, Phys. Plasmas 8 (2001) 447.
 - [21] B. Scott, New J. Phys. 4 (2002) 52.
 - [22] B. Scott, Phys. Letters A 320 (2003) 53.
 - [23] A. B. Hassam, Phys. Fluids 23 (1980) 38.
 - [24] S. Camargo, B. Scott, and D. Biskamp, Phys. Plasmas 3 (1996) 3912.
 - [25] F. Y. Gang, B. D. Scott, and P. H. Diamond, Phys. Fluids B 1 (1989) 1331.
 - [26] B. Scott, H. Biglari, P. W. Terry, and P. H. Diamond, Phys. Fluids B 3 (1991) 51.
 - [27] B. Van Leer, J. Comput. Phys. 32 (1979) 101.
 - [28] P. Colella, J. Comput. Phys. 87 (1990) 171.
 - [29] V. Naulin, New J. Phys. 4 (2002) 28.
 - [30] A. Arakawa, J. Comput. Phys. 1 (1966) 119, repr J. Comput. Phys. 135 (1997) 103.
 - [31] G. E. Karniadakis, M. Israeli, and S. A. Orszag, J. Comput. Phys. 97 (1991) 414.
 - [32] J. M. Albert, P. L. Similon, and R. N. Sudan, Phys. Fluids B 2 (1990) 3032.
 - [33] W. W. Lee, J. Lewandowski, T.-S. Hahm, and Z. Lin, Phys. Plasmas 8 (2001) 4435.
 - [34] T. Dannert and F. Jenko, Comput. Phys. Comm. (2004) in press.

- [35] F. Jenko, W. Dorland, M. Kotschenreuther, and B. N. Rogers, *Phys. Plasmas* 7 (2000) 1904.
- [36] Horton, B. G. Hong, and W. M. Tang, *Phys. Fluids* 31 (1988) 2971.
- [37] J. F. Drake, P. N. Guzdar, and A. B. Hassam, *Phys. Rev. Lett.* 61 (1988) 2205.
- [38] B. Labit and M. Ottaviani, *Phys. Plasmas* 10 (2003) 126.
- [39] J. P. Freidberg, *Ideal Magnetohydrodynamics*, (Plenum Press, New York, 1987).
- [40] A. Hasegawa and L. Chen, *Phys. Fluids* 19 (1976) 1924.

APPENDIX A: SIMPLE CORRESPONDENCE BETWEEN FLUID AND GYROFLUID MODELS

A simple exercise using the most basic reduced MHD interchange model helps gain insight into the relationship between the fluid and gyrofluid models. We start with the two equations written down in the Introduction, writing the electron density equation in terms of a charge density to equalise the units. For reasons which will become clear, we retain the diamagnetic compression effect in the density equation. We also incorporate the profile variation of the thermal state variables, normally acted up solely by ExB advection or magnetic flutter, into the corresponding dependent variables (the only difference this makes is that \mathcal{K} now acts upon the profiles, which is actually somewhat more realistic). The equations are

$$\frac{n_i M_i c^2}{B^2} \frac{d}{dt} \nabla_{\perp}^2 \tilde{\phi} = -T_e \mathcal{K}(\tilde{n}_e) \quad (\text{A1})$$

$$e \frac{d\tilde{n}_e}{dt} = n_e e \mathcal{K}(\tilde{\phi}) - T_e \mathcal{K}(\tilde{n}_e) \quad (\text{A2})$$

with d/dt representing the ExB advective derivative. We now define arbitrarily an auxiliary variable, \tilde{N} , as

$$\tilde{N} e = \tilde{n}_e e - \frac{n_i M_i c^2}{B^2} \nabla_{\perp}^2 \tilde{\phi} \quad (\text{A3})$$

The evolution equation for \tilde{N} is found therefore by subtracting Eqs. (A1,A2),

$$e \frac{d\tilde{N}}{dt} = n_e e \mathcal{K}(\tilde{\phi}) \quad (\text{A4})$$

By inspection with any of the gyrofluid models, we find that N is simply the gyrocenter ion density n_i , with the sole proviso that the background constant parameters for n_e and n_i are equal. This tells us that the MHD formulation for the ExB vorticity is identical to the cold-ion limit of the polarisation density in the gyrofluid model. The relation here is between the polarisation current in the fluid model and the polarisation density in the gyrofluid model. The MHD interchange term $\mathcal{K}(\tilde{n}_e)$ appears properly only if the diamagnetic compression effect is kept in the gyrofluid density equations (i.e., unlike for a fluid model, this effect cannot be neglected in a gyrofluid model). The ExB compression effect in the density cancels out of the interchange effect in the vorticity. However, it is necessary in either model to retain the ExB compression in order to conserve energy. The incidental benefit is to retain the geodesic curvature effect which is the principal mechanism limiting the growth of zonal flows [22].

More detailed accounts of the correspondence between the fluid and gyrofluid models may be found elsewhere [3, 9, 19].

FIGURE CAPTIONS

Figure 1. Kinetic shear Alfvén damping rates versus normalised beta, electron mass, and Landau damping closure coefficient. In the leftmost two frames the blue line (whose peak is toward lower $\hat{\beta}$ values and higher $\hat{\mu}$ values) gives the kinetic dispersion relation using the method of Ref. [34]. The calibration works in the $\beta_e \gg \mu_e$ regime and yields qualitatively similar behaviour elsewhere, though the details of the peaks can only be captured with a kinetic model.

Figure 2. Transport of ITG turbulence found by GEM (triangles, one per sample as described in the text), compared to the gyrokinetic fit from Ref. [1]. The transport diffusivity, χ_i , calculated temporally as described in the text, is normalised to a nominal value of $\chi_0 = \rho_s^2 c_s / L_n$. The fact that the groups of points from four decaying runs overlap well indicates the transport to be temporally local.

Figure 3. Transport spectra and density morphology in core ETG turbulence in the linear (left) and saturated (right) phases, as described in the text. Lines marked 'n' and 'N' are for the particle flux, where it is positive or negative, respectively. Lines marked 't' and 'i' are for the electron and ion conductive heat fluxes, respectively. The scales are normalised to ρ_s ; multiply $\{x, y\}$ and divide k_y by 60.6 to obtain them in terms of ρ_e .

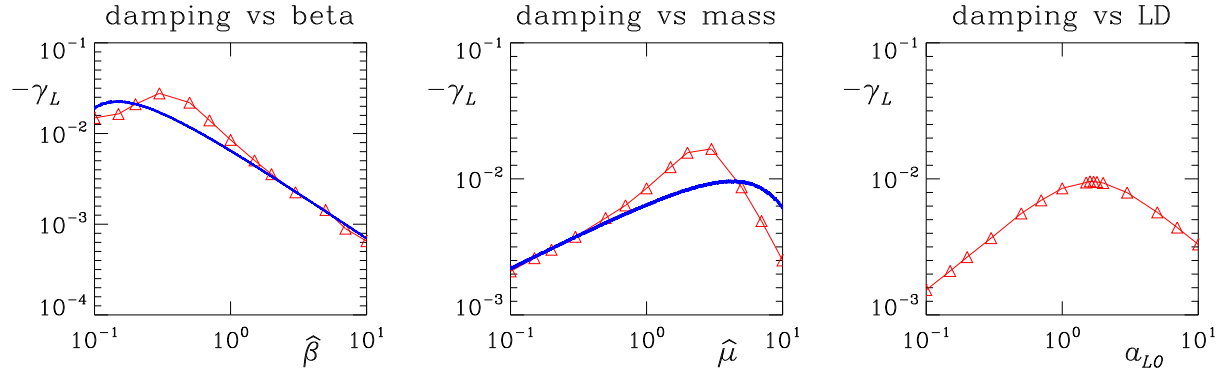


FIG. 1: Kinetic shear Alfvén damping rates versus normalised beta, electron mass, and Landau damping closure coefficient. In the leftmost two frames the blue line (whose peak is toward lower $\hat{\beta}$ values and higher $\hat{\mu}$ values) gives the kinetic dispersion relation using the method of Ref. [34]. The calibration works in the $\beta_e \gg \mu_e$ regime and yields qualitatively similar behaviour elsewhere, though the details of the peaks can only be captured with a kinetic model.

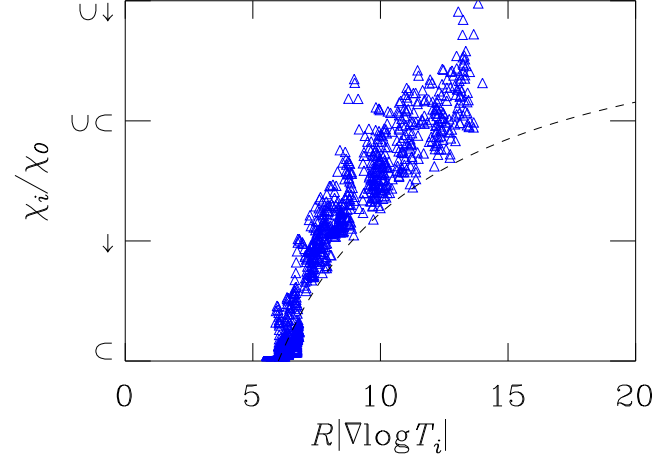


FIG. 2: Transport of ITG turbulence found by GEM (triangles, one per sample as described in the text), compared to the gyrokinetic fit from Ref. [1]. The transport diffusivity, χ_i , calculated temporally as described in the text, is normalised to a nominal value of $\chi_0 = \rho_s^2 c_s / L_n$. The fact that the groups of points from four decaying runs overlap well indicates the transport to be temporally local.

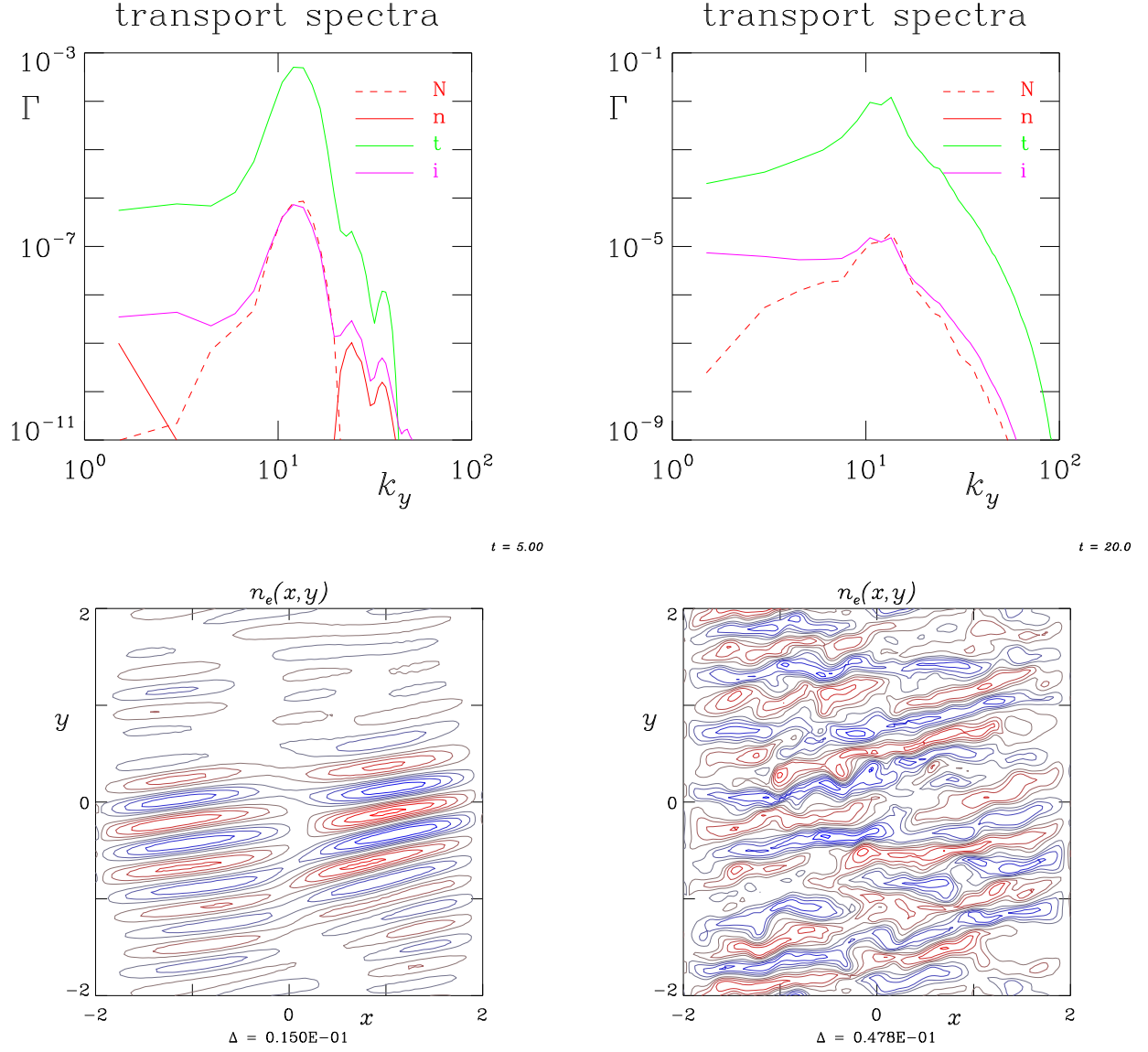


FIG. 3: Transport spectra and density morphology in core ETG turbulence in the linear (left) and saturated (right) phases, as described in the text. Lines marked 'n' and 'N' are for the particle flux, where it is positive or negative, respectively. Lines marked 't' and 'i' are for the electron and ion conductive heat fluxes, respectively. The scales are normalised to ρ_s ; multiply $\{x, y\}$ and divide k_y by 60.6 to obtain them in terms of ρ_e .